

### INFORMATION TO USERS

This reproduction was made from a copy of a document sent to us for microfilming. While the most advanced technology has been used to photograph and reproduce this document, the quality of the reproduction is heavily dependent upon the quality of the material submitted.

The following explanation of techniques is provided to help clarify markings or notations which may appear on this reproduction.

1. The sign or "target" for pages apparently lacking from the document photographed is "Missing Page(s)". If it was possible to obtain the missing page(s) or section, they are spliced into the film along with adjacent pages. This may have necessitated cutting through an image and duplicating adjacent pages to assure complete continuity.
2. When an image on the film is obliterated with a round black mark, it is an indication of either blurred copy because of movement during exposure, duplicate copy, or copyrighted materials that should not have been filmed. For blurred pages, a good image of the page can be found in the adjacent frame. If copyrighted materials were deleted, a target note will appear listing the pages in the adjacent frame.
3. When a map, drawing or chart, etc., is part of the material being photographed, a definite method of "sectioning" the material has been followed. It is customary to begin filming at the upper left hand corner of a large sheet and to continue from left to right in equal sections with small overlaps. If necessary, sectioning is continued again—beginning below the first row and continuing on until complete.
4. For illustrations that cannot be satisfactorily reproduced by xerographic means, photographic prints can be purchased at additional cost and inserted into your xerographic copy. These prints are available upon request from the Dissertations Customer Services Department.
5. Some pages in any document may have indistinct print. In all cases the best available copy has been filmed.

**University  
Microfilms  
International**

300 N. Zeeb Road  
Ann Arbor, MI 48106

-

**Grayson, Matthew Aaron**

GEOMETRY AND GROWTH IN THREE DIMENSIONS

*Princeton University*

PH.D. 1983

University  
Microfilms  
International

300 N. Zeeb Road, Ann Arbor, MI 48106



PLEASE NOTE:

In all cases this material has been filmed in the best possible way from the available copy. Problems encountered with this document have been identified here with a check mark .

1. Glossy photographs or pages \_\_\_\_\_
2. Colored illustrations, paper or print \_\_\_\_\_
3. Photographs with dark background \_\_\_\_\_
4. Illustrations are poor copy \_\_\_\_\_
5. Pages with black marks, not original copy \_\_\_\_\_
6. Print shows through as there is text on both sides of page \_\_\_\_\_
7. Indistinct, broken or small print on several pages \_\_\_\_\_
8. Print exceeds margin requirements \_\_\_\_\_
9. Tightly bound copy with print lost in spine
10. Computer printout pages with indistinct print \_\_\_\_\_
11. Page(s) \_\_\_\_\_ lacking when material received, and not available from school or author.
12. Page(s) \_\_\_\_\_ seem to be missing in numbering only as text follows.
13. Two pages numbered \_\_\_\_\_. Text follows.
14. Curling and wrinkled pages \_\_\_\_\_
15. Other \_\_\_\_\_

University  
Microfilms  
International

.

GEOMETRY AND GROWTH IN THREE DIMENSIONS

by

Matthew Aaron Grayson

A thesis  
presented to Princeton University  
in partial fulfillment of the  
requirements for the degree of  
Ph.D.  
in  
Mathematics

Princeton, New Jersey, 1983

© Matthew Aaron Grayson, 1983

To my Mother and Father

## ABSTRACT

We investigate the connection between geometry of three manifolds and the combinatorics of their fundamental groups, e.g., growth functions. In most cases, we derive explicit expressions for the growth function.

We look at orbifolds whose fundamental groups are generalizations of right angle reflection groups, and see a strong connection between the geometry of their fundamental domain, and the growth functions of their fundamental groups. In particular, the growth function depends only on the fundamental domain, and not on the choice of an identification of its boundary. Important examples are the alternating link complements in the three-sphere. The growth functions of their fundamental groups depend only on the number of crossings.

We also look at Solv geometry and its geodesics, and the combinatorics of the fundamental groups of torus bundles over the circle. We find the closed geodesics representing the free homotopy classes in torus bundles. In many classes, there are a number of different lengths of closed geodesics. Each length has a unique representative up to isometry.

We look at the geometry  $SL_2$ , which models non-trivial Seifert fiber spaces with hyperbolic base orbifolds. We show that there is a group whose growth restricted to a subgroup is irrational.

## ACKNOWLEDGEMENTS

Bill Thurston turns out another graduate student. I don't see why he does it. We bother him, ask him dumb questions, follow him to Boulder, ask him for letters of recommendation, and mostly, fail to understand what he's trying to say. If there were anything we could do (aside from random acknowledgements) to even the score, ....

Thanks to Jim Cannon for getting me to work on growth functions the day after my generals, and for discovering many of their mysterious properties.

Many thanks to Rachel, Nathaniel, Dylan, and Emily for making life in Princeton more normal, and often pleasant, and thanks to Lee for making it weird.

And thanks to the I.B.M. 3081. It types alot faster than I do, but makes just as many mistakes.

## CONTENTS

ABSTRACT . . . . .	ii
ACKNOWLEDGEMENTS . . . . .	iii

Chapter

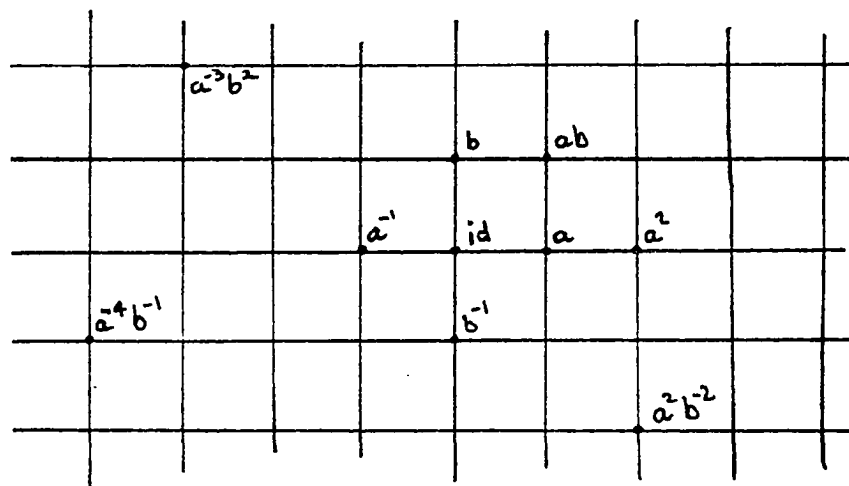
	<u>page</u>
I. INTRODUCTION . . . . .	1
Some Interesting Facts About Growth Functions . . . . .	7
Proposition . . . . .	7
Proposition . . . . .	8
Proposition . . . . .	10
II. GROUPS GENERATED BY RIGHT-ANGLED POLYHEDRA . . . . .	12
The Main Theorem . . . . .	35
The Technical Lemma . . . . .	36
Lemma . . . . .	36
The Face Coefficient . . . . .	37
The Edge Coefficient . . . . .	43
The Vertex Coefficient . . . . .	47
The Proof of the Main Theorem . . . . .	49
The Growth of Alternating Link Complements . . . . .	52
Theorem . . . . .	53
Theorem . . . . .	58
III. SOLV GEOMETRY AND TORUS BUNDLES . . . . .	60
Curvature . . . . .	61
Geodesics . . . . .	62
Lemma . . . . .	75
Theorem . . . . .	78
Geodesics in Torus Bundles . . . . .	79
The Solv Geometry Structure on Torus Bundles . . . . .	79
Theorem . . . . .	80
Proposition . . . . .	81

IV.	THE GROWTH OF TORUS BUNDLES . . . . .	86
	The Limiting Case . . . . .	86
	Types in a Plane . . . . .	88
	Lemma . . . . .	90
	The Simplification . . . . .	95
V.	SL(2,R) AND SEIFERT FIBRE SPACES . . . . .	105
	Isometries of $SL_2$ . . . . .	105
	An Irrational Subgroup . . . . .	108
	The Fundamental Spiral . . . . .	109
	Theorem . . . . .	110
	The Dual Reduction of an Octagon Packing . . . . .	112
	Lemma . . . . .	112
	Lemma . . . . .	115
	BIBLIOGRAPHY . . . . .	119

## Chapter I

### INTRODUCTION

Look at a torus. It is the quotient of the plane by  $Z+Z$ . It also has a flat geometric structure. Look at its fundamental group a different way. Take  $Z+Z$  with the standard generators. Given a group with generators, we can form the graph of the group. The vertices of the graph  $\Gamma$  are the elements of the group  $G$ . Two vertices,  $x$  and  $y$ , are joined by an edge if there is a generator  $g$  such that  $gx=y$ . With the standard generators, the graph of  $Z+Z$  looks like graph paper:



Consider the graph metric which assigns length one to each edge. We can now ask about the sphere of radius  $r$ . It consists of those ele-

ments of  $G$  whose minimal representations as words in the generating set have length  $r$ .

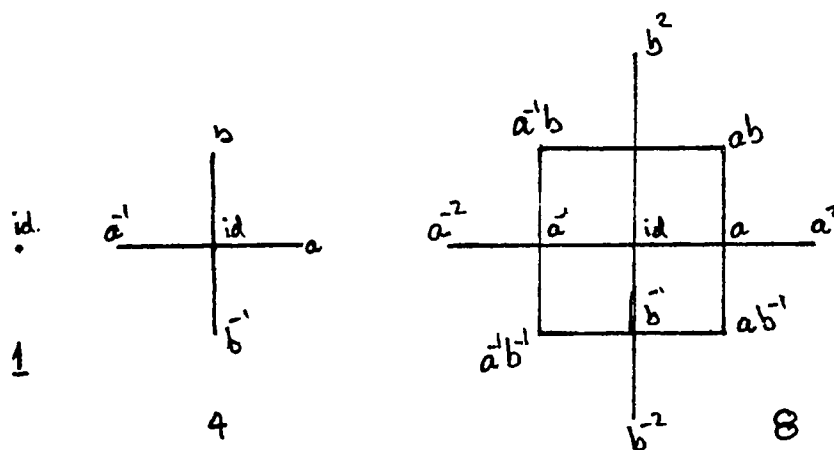
Let  $a_i$  = the number of group elements of minimal length  $i$ . This is called the growth sequence of  $G$  with chosen generators. The generating function for this sequence we will call the growth function

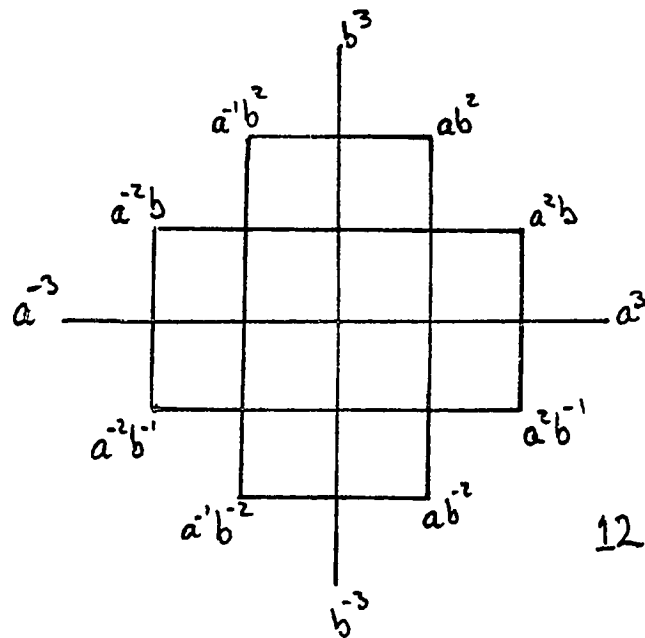
$$\mathcal{G}(s) = \sum_{i=0}^{\infty} a_i s^i$$

We can also look at the number,  $b_i$ , of elements which have minimal representations of length less than or equal to  $i$ . We get

$$\mathcal{B}(s) = (1-s) \sum_{i=0}^{\infty} b_i s^i.$$

Back to the torus. We can write down the growth function by inspection.





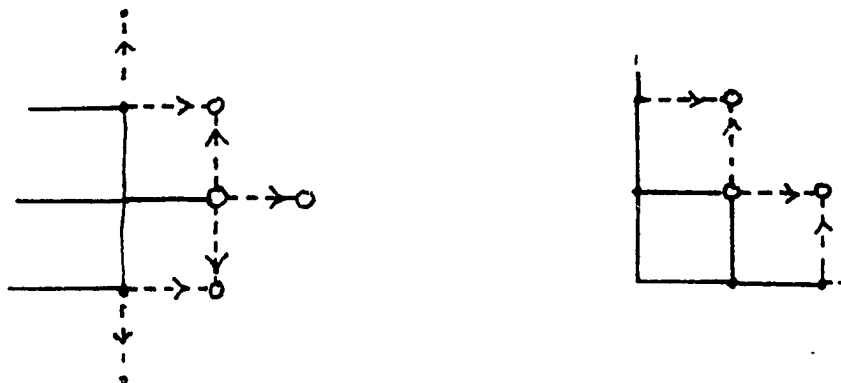
$$(s) = 1 + 4s + 8s^2 + 12s^3 + 16s^4 + \dots + 4ns^n + \dots$$

or,

$$\left( \frac{1+s}{1-s} \right)^2$$

But what is happening?

On the sphere of radius  $r$  in this graph, there are two kinds of behaviour. Some points have a unique predecessor, others have two. Call them type 1 and type 2 points. A type one point contributes one type one point and half of two type 2 points in the next layer. A type 2 point has a half share in each of two type 2 points in the next layer.



If a layer has  $x$  type 1 points and  $y$  type 2 points, then the next layer will have

$$\begin{pmatrix} 1 & 0 \\ 1 & 1 \end{pmatrix} \begin{pmatrix} x \\ y \end{pmatrix} = \begin{pmatrix} x \\ x+y \end{pmatrix} \begin{matrix} \text{type 1} \\ \text{type 2} \end{matrix}$$

Note the similarity between the characteristic polynomial of this matrix and the denominator of the growth function.

There are a lot of manifolds with fundamental groups. An interesting subcategory is the manifolds with geometric structures, that is, manifolds whose fundamental groups are represented as discrete subgroups of the group of isometries of some geometry. See Thurston[12] or Scott[10].

Our Purpose is to study the relationship between geometry and combinatorics, e.g., growth functions, for geometric three dimensional manifolds. Much is already known about this relationship. Milnor[ 8 ] has shown that a compact negatively curved manifold's fundamental group has exponential growth for any set of generators. That is, there exist constants  $C>0$  and  $\alpha>1$  such that

$$a_i > Ce^{\alpha i}$$

We say that a sequence has polynomial growth if there exist constants  $N$  and  $n$  such that

$$a_i < Ni^n.$$

Gromov[ 6 ] has shown that the growth of the fundamental group is polynomial iff the fundamental group has a nilpotent subgroup of finite index.

Wolf[13] has shown that for finitely generated solvable groups, one can determine whether the growth is polynomial or exponential. In particular, the growth of the fundamental group of a torus bundle over a circle is exponential iff the monodromy is Anosov.

The rationality question is also interesting. Cannon[5] has shown that the growth function for the fundamental group of a hyperbolic manifold is rational, regardless of the choice of generating set.

Benson[1] has shown the same for Euclidean manifolds.

In this thesis, we investigate some classes of examples of geometric three-manifolds and their growth functions. For this purpose, it is sometimes necessary to pick a preferred generating set to render the computations bearable.

Chapter 2 deals with groups which are generalizations of hyperbolic right angle reflection groups. The growth functions depend only on some simple combinatorial data about the fundamental domain. An application to alternating links is given at the end of the chapter. An alternating projection gives rise to a set of generators for the fundamental group of the complement of the link in the three-sphere. The growth function for this presentation depends only on the number of crossings of the link under that projection.

Chapter 3 is an excursion into one of the eight three-manifold geometries, Solv. This geometry models the torus bundles over the circle with Anosov monodromy. We find, among other things, the closed geodesics representing the free homotopy classes of a given torus bundle. This work stems from an attempt to understand spheres in the group graph by looking at metric spheres in the universal cover. The behaviour of geodesics mimics closely the growth of words in the fundamental groups of torus bundles.

Chapter 4 looks at the actual growth functions of torus bundles with Anosov monodromy.

Chapter 5 takes a look at another geometry, that modelled on  $SL_2\mathbb{R}$ , and the strange behaviour of the graphs of fundamental groups of circle bundles over surfaces.

## 1.1 SOME INTERESTING FACTS ABOUT GROWTH FUNCTIONS

Suppose that we have groups  $F$  and  $G$  with generating sets  $\{f_i\}$ , and  $\{g_j\}$ , respectively. Let  $f(s)$  and  $g(s)$  denote the growth functions of  $F$  and  $G$  with these generators, then

### 1.1.1 Proposition

Let  $H$  be the direct sum of  $F$  and  $G$  with generators  $\{(f_i, id)\} \{(id, g_j)\}$ . Then the growth function for  $H$ ,  $h(s)$  is given by:

$$h(s) = f(s)g(s).$$

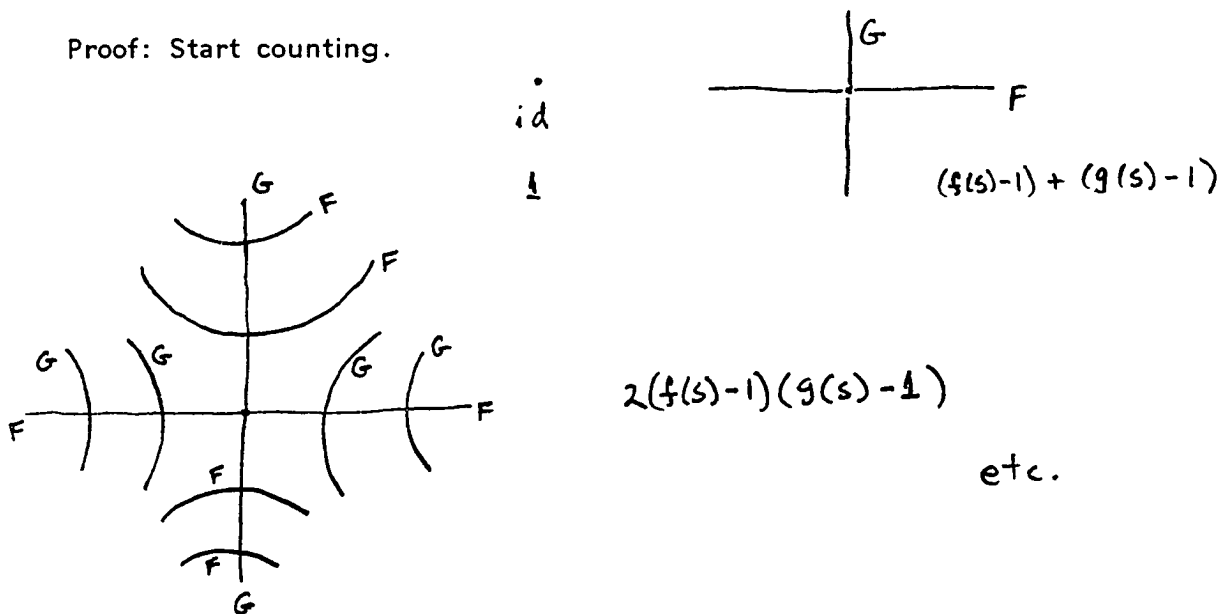
Proof: The length of a word  $(x, y)$  in  $H$  is the sum of the length of  $x$  in  $F$  plus the length of  $y$  in  $G$ . The proposition follows immediately.

## 1.1.2 Proposition

Let  $H$  be the free product of  $F$  and  $G$ , then

$$h(s) = \frac{f(s)g(s)}{f(s) + g(s) - f(s)g(s)}$$

Proof: Start counting.



so:

$$h(s) = 1 + (f(s)-1) + (f(s)-1)(g(s)-1) + (f(s)-1)^2(g(s)-1) + (f(s)-1)^2(g(s)-1)^2 + \dots \\ + (g(s)-1) + (g(s)-1)(f(s)-1) + (g(s)-1)^2(f(s)-1) + (g(s)-1)^2(f(s)-1)^2 + \dots$$

Which simplifies to the desired formula.

Some useful consequences, which can be arrived at easily by other means, are the growth functions of the free groups, and the free abelian groups. The growth function of the free abelian group of rank  $n$  is

$$\left(\frac{1+s}{1-s}\right)^n$$

The growth function for the free group of rank  $n$  is

$$\frac{1+s}{1-(2n-1)s}$$

Now suppose that the growth function really is rational, then we can see that the denominator must have constant term 1. If not, then the sequence of coefficients of the power series for the growth function would not have integral coefficients. Therefore, the roots of the denominator, and hence the poles of the growth function, are located at the inverses of algebraic integers.

### 1.1.3 Proposition

The exponential growth of the coefficients of the power series of a rational function is determined by the norm of the inverse of the smallest root of the denominator. (Assuming that the numerator and the denominator have no roots in common).

Sketch of Proof: This is fairly easy. One good way to see it is by constructing a matrix which gives the terms in the power series as follows:

M has 1's on the super diagonal, and the bottom row has the coefficients of the denominator written in decreasing order, that is, if

$$g(s) = p(s)/q(s)$$

and

$$q(s) = q_0 + q_1s + q_2s^2 + \dots + q_ns^n,$$

then the bottom row of M is

$$q_n, q_{n-1}, \dots, q_1, q_0.$$

Now if  $V$  is a vector consisting of  $n+1$  consecutive terms in the sequence of coefficients, say from  $a_i$  to  $a_{i+n}$ , then  $(M)V$  will be the vector of coefficients from  $a_{i+1}$  to  $a_{i+n+1}$ . But, as  $M$  is in Rational Canonical Form, the characteristic polynomial of  $M$  is

$$q_n + q_{n-1}s + \dots + q_1s^{n-1} + q_0s^n.$$

So the largest eigenvalue of  $M$  is the inverse of the smallest root of  $q(s)$ . It suffices to show that the vector  $V$  does not lie in a subspace spanned by eigenvectors with smaller eigenvalues. If it did, then we could factor the smallest root out of both the numerator and denominator, since we could remove the root in question and still generate the desired sequence of vectors having integral coefficients.

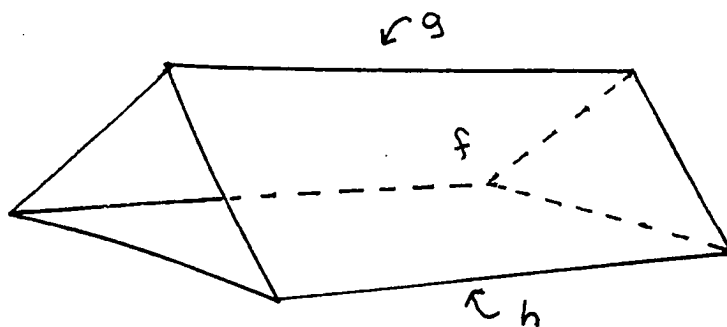
## Chapter II

### GROUPS GENERATED BY RIGHT-ANGLED POLYHEDRA

Let  $P$  be a polyhedron, that is  $P$  is a two sphere with a cellular subdivision into faces, edges and vertices. We require  $P$  to satisfy certain combinatorial criteria.

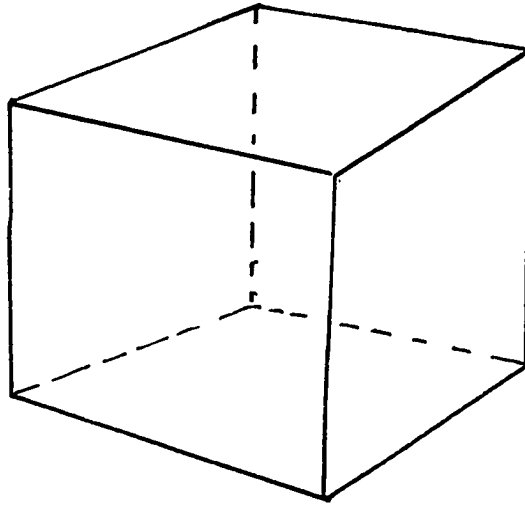
1. Each face of  $P$  has at least four edges.
2. Each vertex of  $P$  is contained in exactly three edges.
3. Each edge of  $P$  is contained in exactly two distinct faces.
4. Each three-cycle of faces has a common vertex.
5. No two faces meet along more than one edge.

A three-cycle of faces is a collection of three faces with the property that each face has an edge in common with each of the other two.

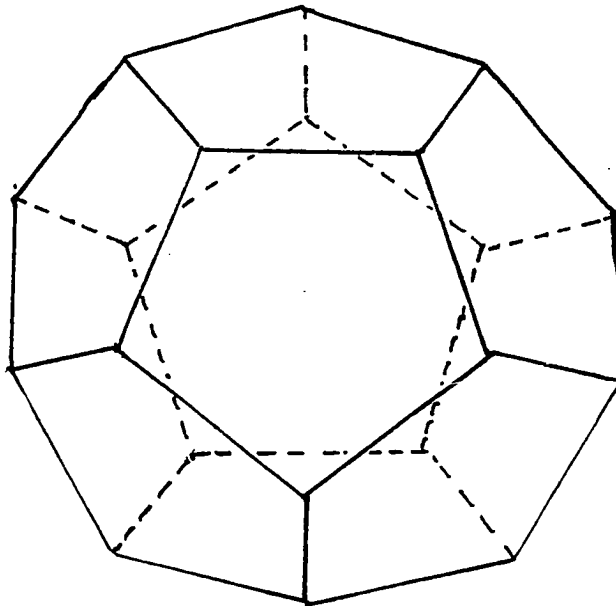


Three cycle  $f-g-h$ .

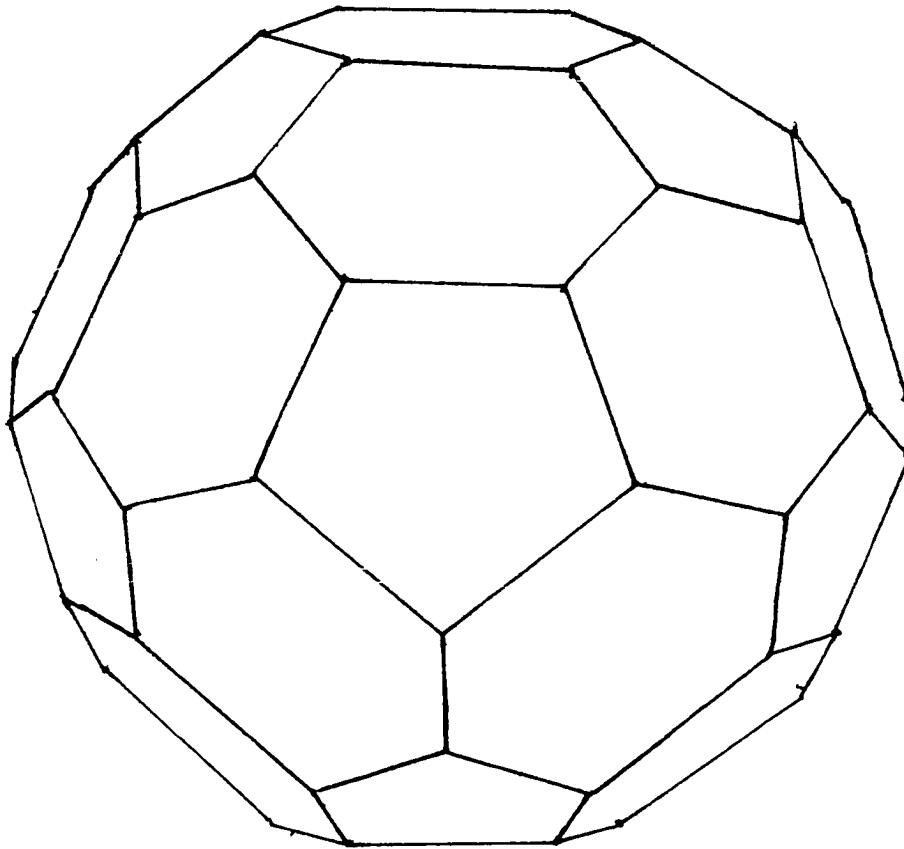
Example: Cube



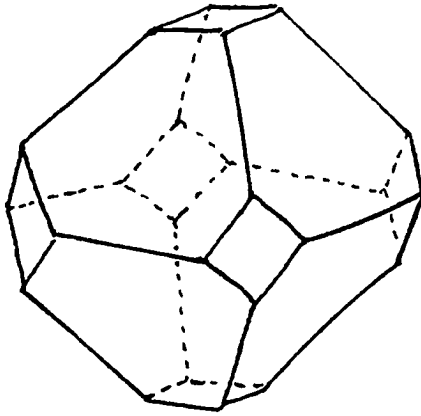
Example: Dodecahedron.



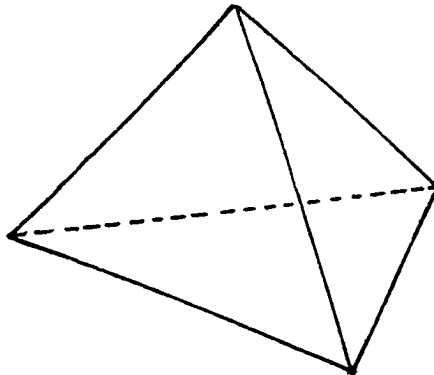
Example: Soccer Ball



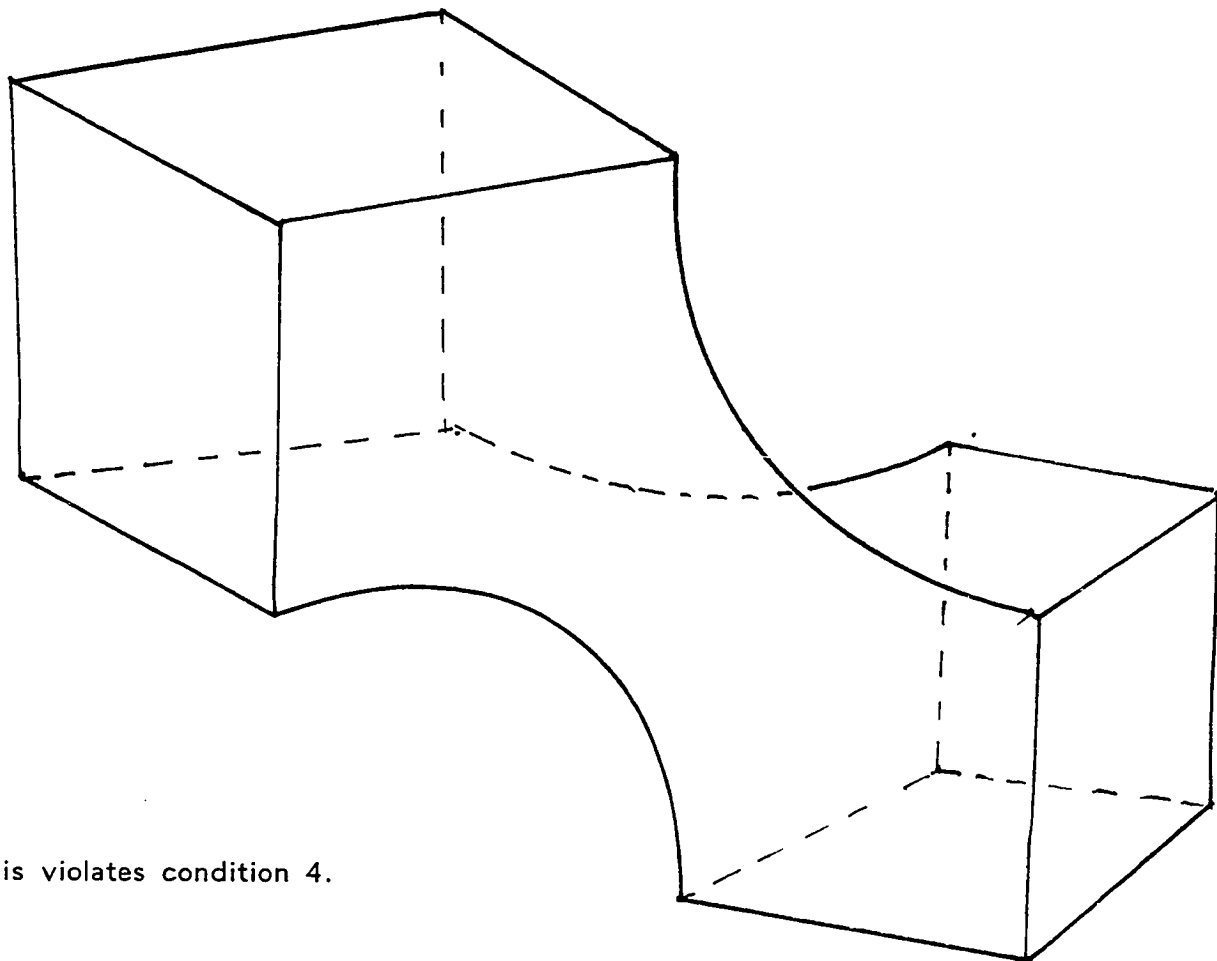
Example: Truncated Octahedron



Non-example: Tetrahedron

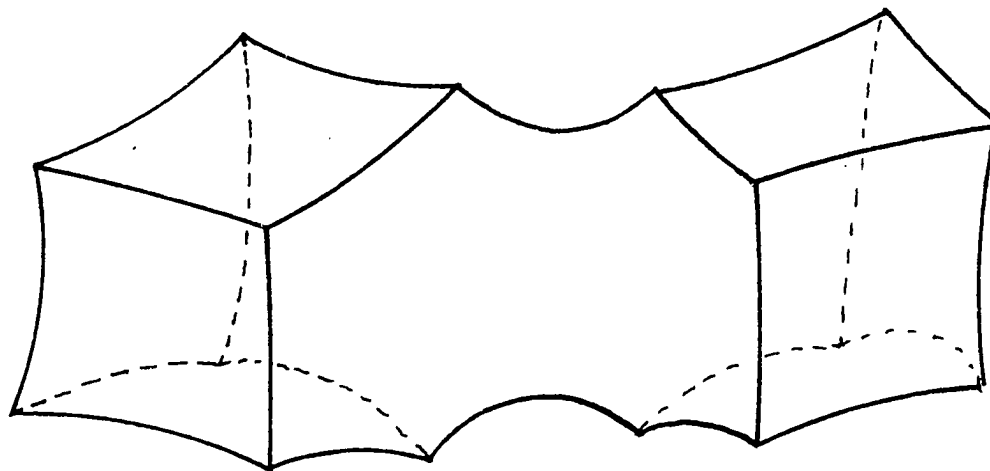


Non-example: Connected sum of Two Cubes at a Vertex



This violates condition 4.

Non-example: Connected Sum of Two Cubes along an Edge



This violates condition 5.

From now on, we will assume that all polyhedra satisfy the above combinatorial conditions.

These combinatorial criteria are designed to include both hyperbolic and euclidean polyhedra, as well as some hybrids which can exist in neither geometry as polyhedra with planar faces and right dihedral angles. These hybrids, such as the truncated octahedron, are interesting, because they exhibit characteristics of both geometries in their combinatorics and growth.

If the polyhedron  $P$  had a geometric structure, we could talk about the dihedral angles at the edges. As it is, if we want a group acting on  $R^3$  with fundamental domain  $P$ , then we have to specify combinatorial conditions on the generators of the group to ensure that, in the universal cover,  $P$  acts as if it does indeed have right dihedral angles.

First choose a subset of the faces of  $P$  and designate them as infinite. All edges and vertices of an infinite face are also infinite. The remaining cells are called finite. The group will ignore infinite cells. From now on, any cell will be assumed finite unless otherwise specified. Furthermore, we can make the following change in  $P$ . If a finite face has two or more adjacent infinite edges, then we can replace them with a single infinite edge. This makes for some strange looking polyhedra, but it does not affect the combinatorics of the group (to be defined).

Next choose a pairing of the finite faces of  $P$ . That is, to every finite face  $f$  of  $P$ , assign a (possibly the same) finite face  $g$  and an isomorphism

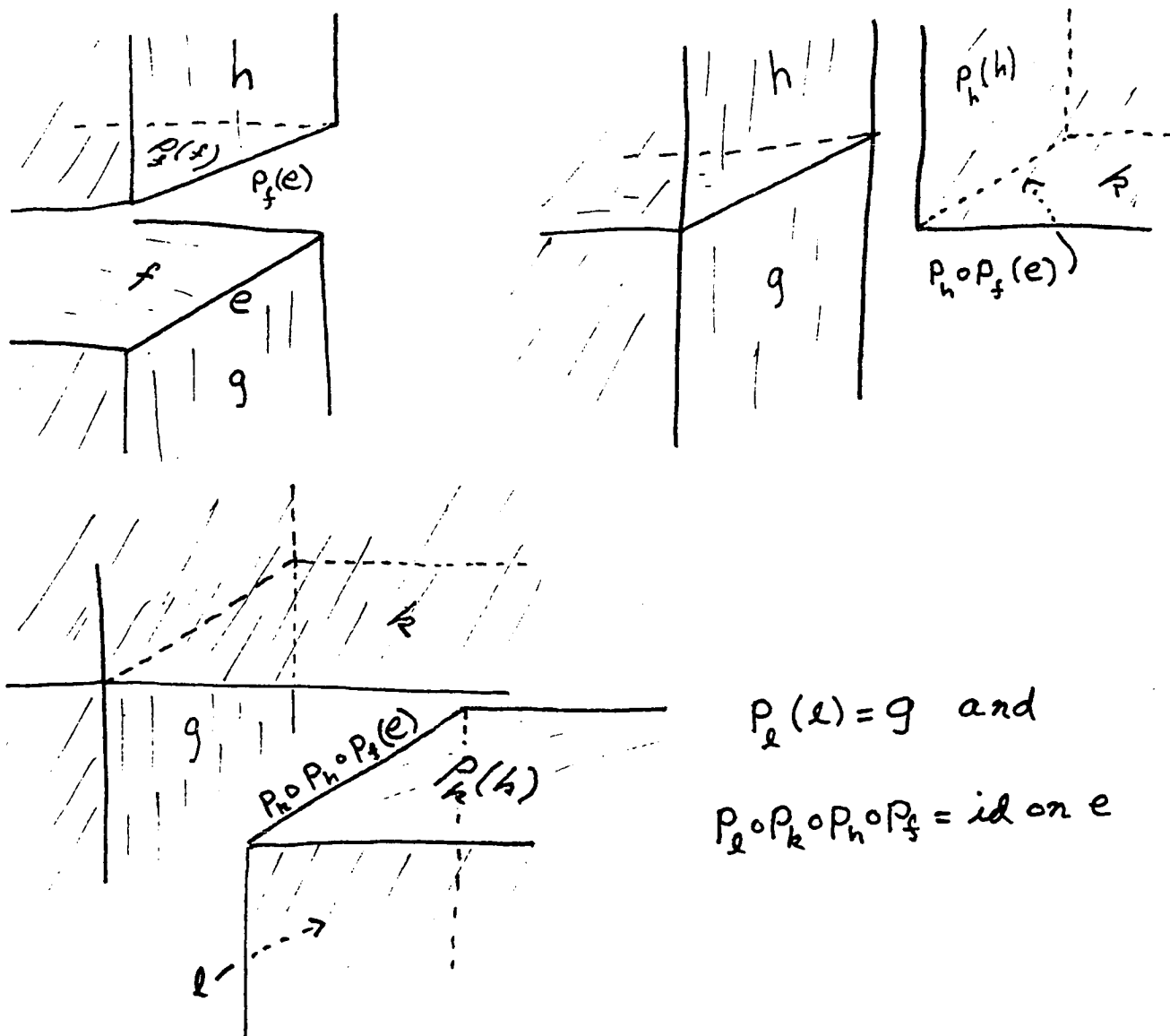
$$p_f: f \rightarrow g.$$

We require that

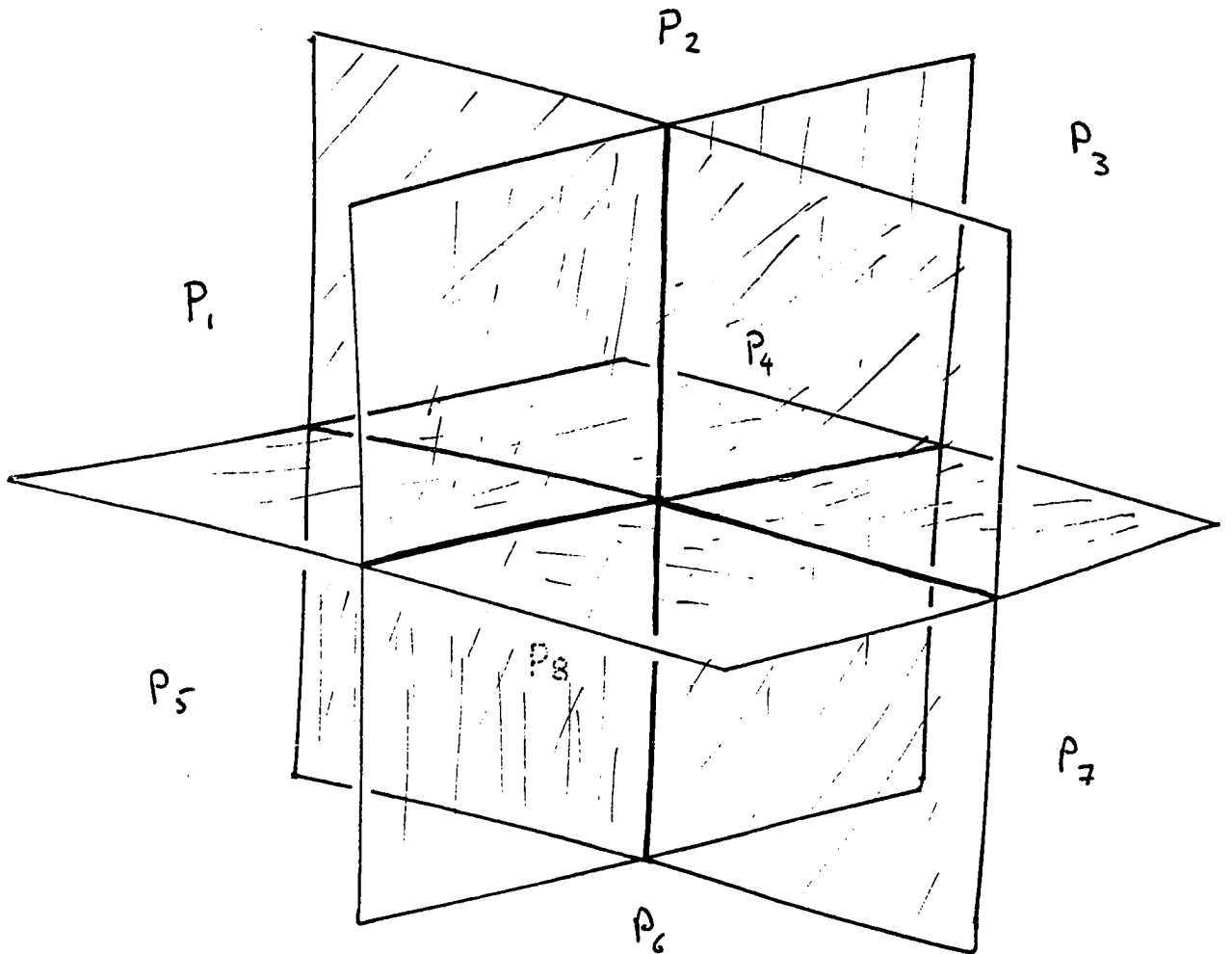
$$p_g: g \rightarrow f \text{ and } p_g \circ p_f = \text{id}.$$

Furthermore,  $p_f$  must match finite edges and vertices to finite edges and vertices, as well as infinite to infinite. It may be orientation preserving or reversing.

Now comes the right angle condition. The order of the orbit of any edge under the  $p$ 's must be no more than four. The order of the orbit of a vertex must be no more than eight. At each finite edge, we require the following picture:



Similarly, at finite vertices, we must have:



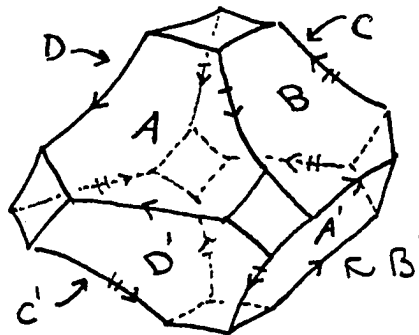
ALL FACE PAIRINGS MUST BE CONSISTENT  
WITH THIS PICTURE.

Example: Let  $P$  be any compact hyperbolic polyhedron with right dihedral angles and let the face pairings be given by reflection in each face.

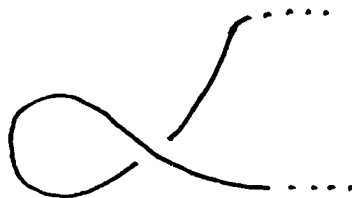
Example: Let  $P$  be a regular cube and let opposite faces be identified by translation.

Example: Let  $P$  be the truncated octahedron. Let the squares be infinite, and identify the remaining faces in the pattern given below.

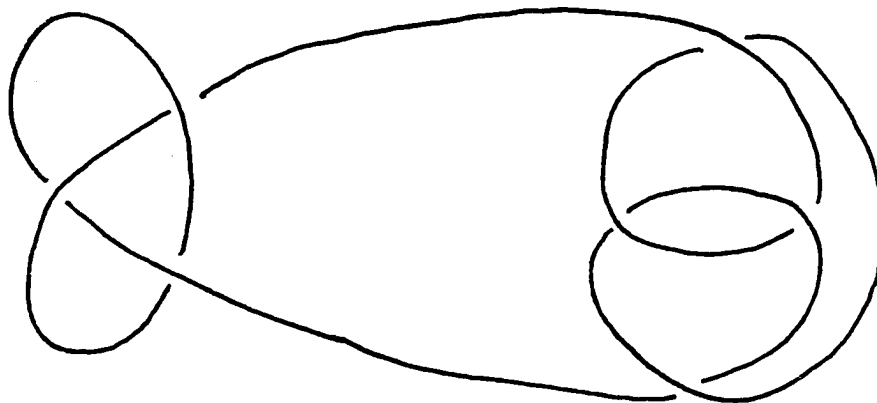
This identification yields the complement in  $S^3$  of the Whitehead link. See Thurston [12].



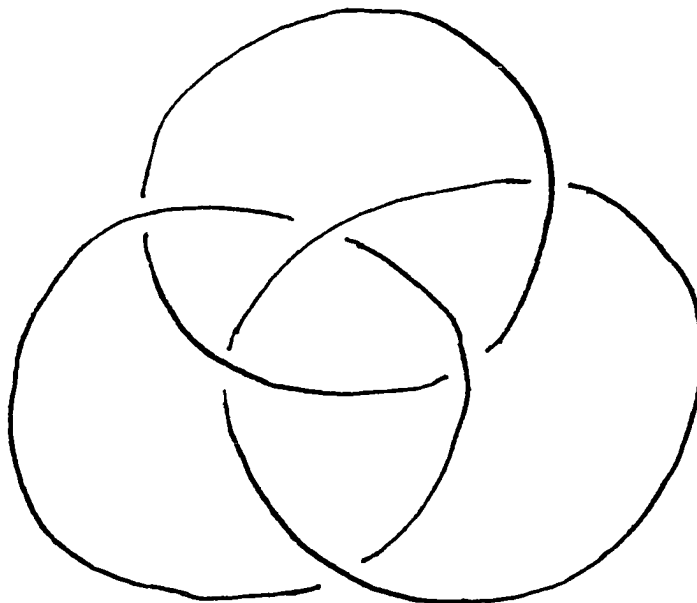
Example: Let  $k$  be any prime alternating link without trivial twists. That is, nothing of the form:

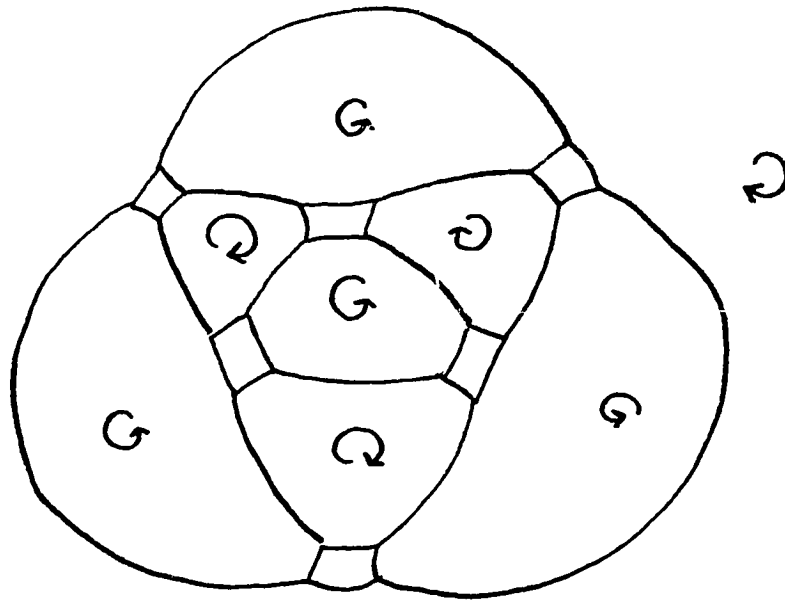


or:

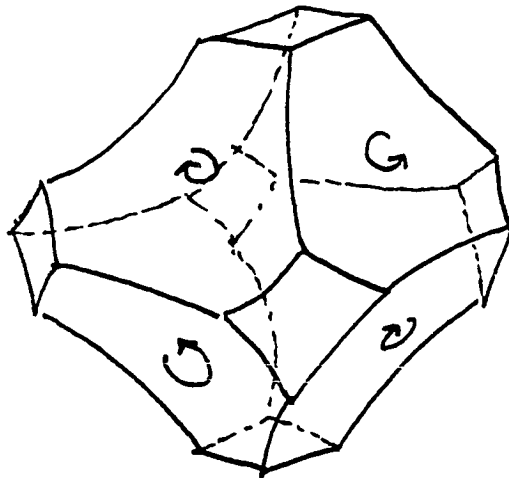


Now, replace each crossing in the projection with a tiny infinite square. This is  $P$ . Let the face pairings be given by reflection composed with a rotation by one edge. The direction of rotation on each face is chosen to mesh with its neighbors. For instance, if  $k$  is the Borromean Rings:



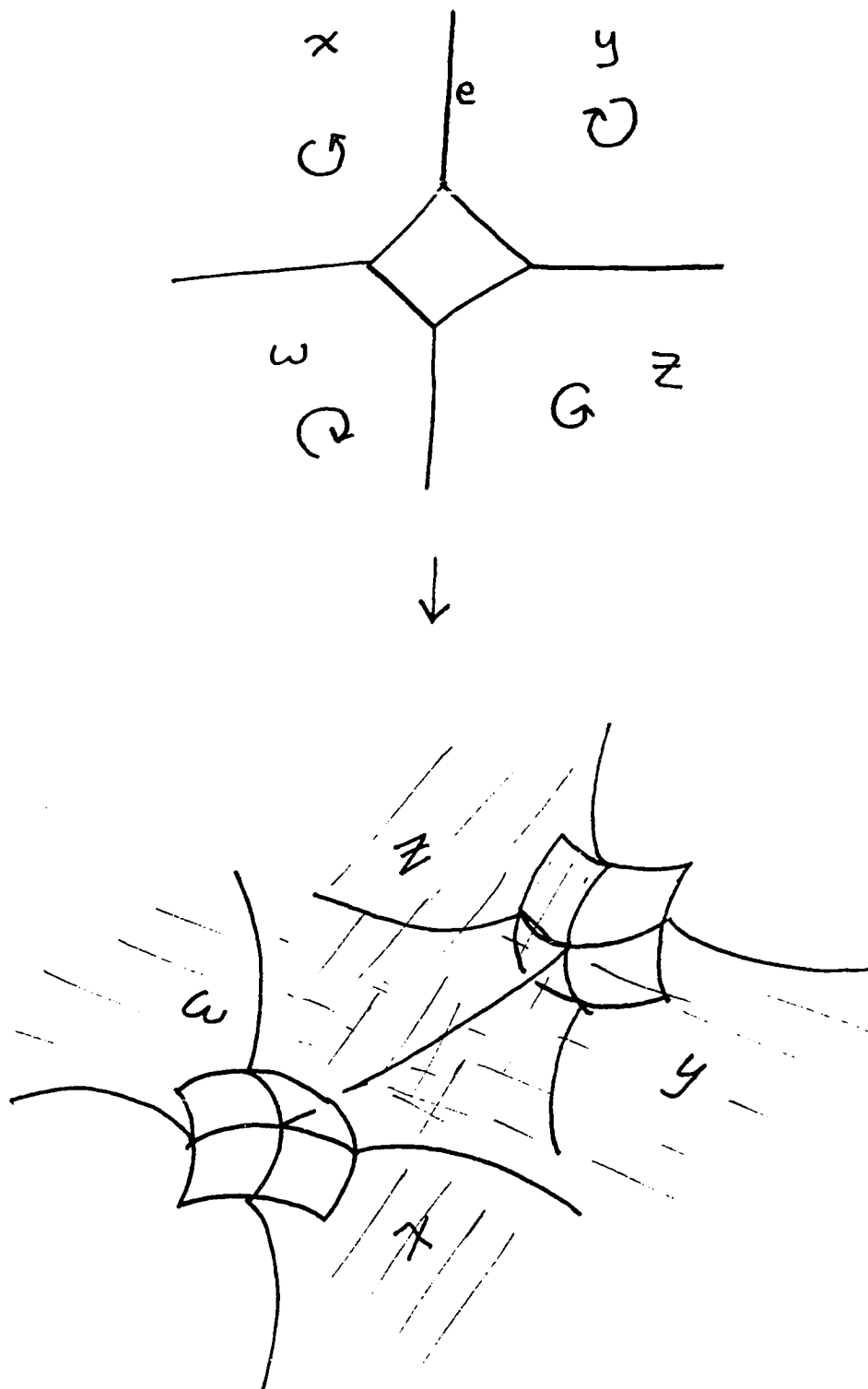


or:



Exercise: Verify that this pairing is admissible. Note that no vertex is finite, so it suffices to verify the edge conditions.

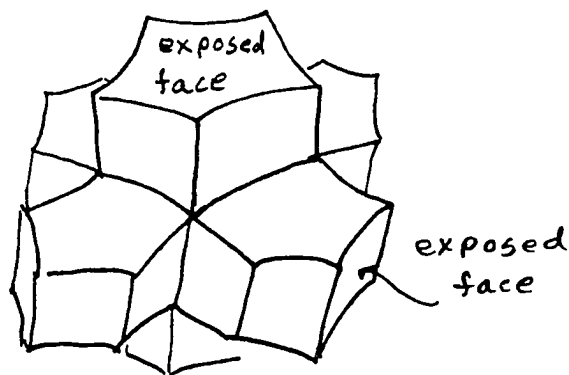
See Menasco [7].



We now use the face pairing maps to build the universal cover of our polyhedron  $P$  as if it had right dihedral angles. The consistency conditions on the face pairings guarantee that, combinatorially, this can be done. Locally, we can build a cell complex with four faces meeting every finite edge, and six edges meeting every finite vertex. We will see that every edge in the cell complex has at first one, then three, then four polyhedra adjacent to it as we build the universal cover. Our goal is to study the group  $G$  of deck transformations of the universal cover of  $P$ , and to calculate the growth function of this group. If we pick one copy of  $P$  and identify it with the identity element of  $G$ , then we can identify words in  $G$  with copies of  $P$  in the universal cover. Here is what happens.

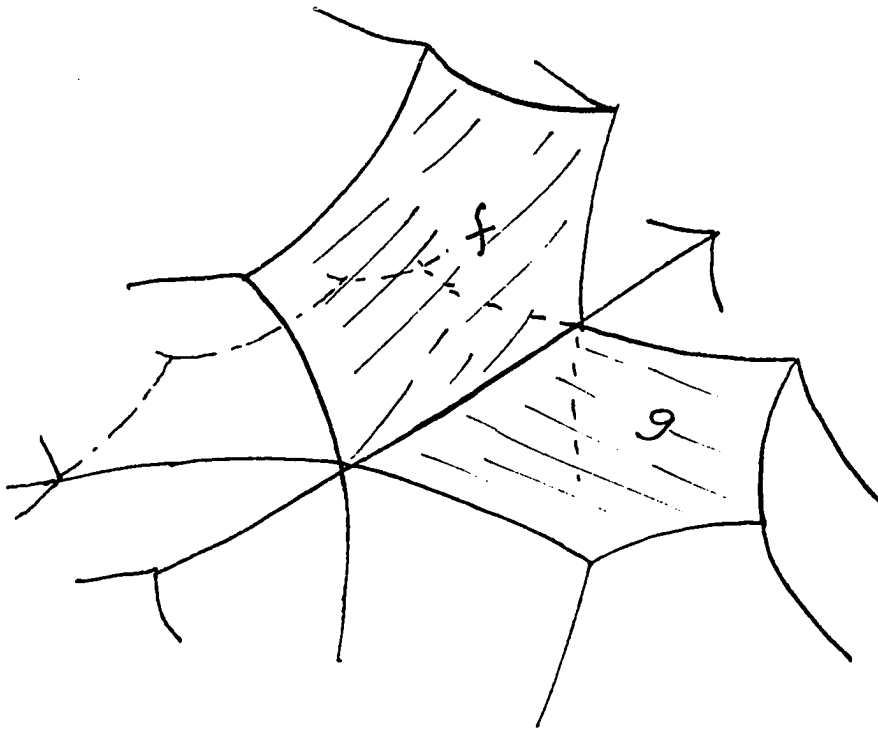
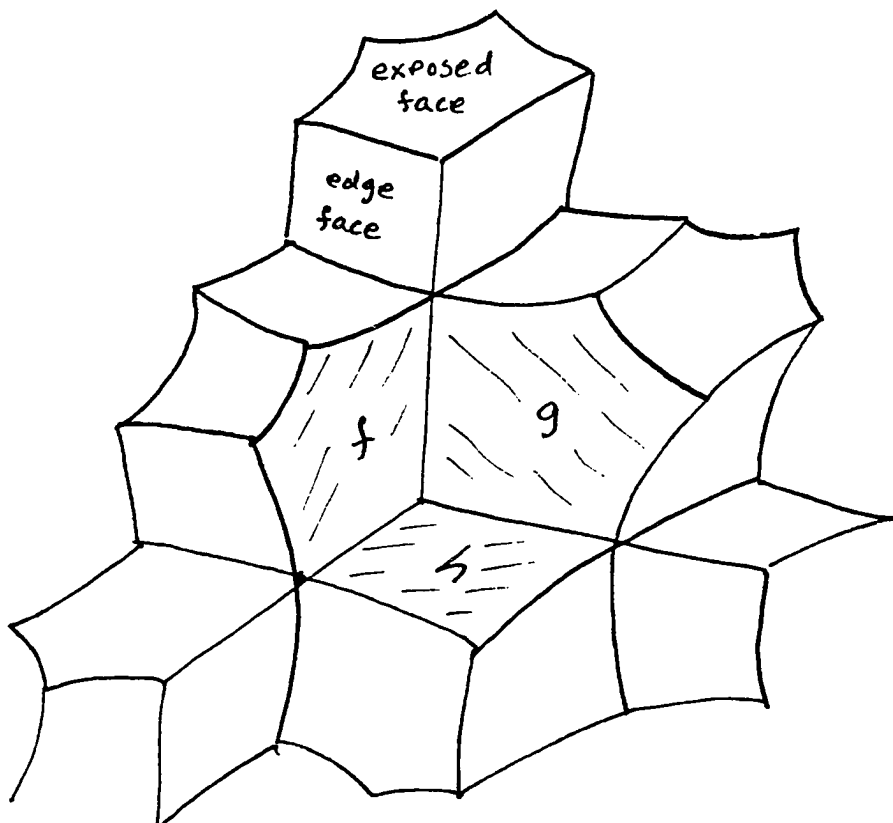
Pick  $B_0 = P$  to represent the identity element. Each generator  $p_f$  corresponds to a copy of  $P$  glued to  $B_0$  at the appropriate finite face. In general,  $B_{i+1}$  is obtained from  $B_i$  by gluing copies of  $P$  to all finite faces on the boundary of  $B_i$ . If an edge on the boundary of  $B_i$  touches one polyhedron, then it will touch three in layer  $B_{i+1}$ . If it touches three in layer  $B_i$ , then the right angle allows only one more to be added at that edge. These polyhedra correspond to the words in  $G$  of length  $i+1$  as obtained by multiplying each word of length  $i$  by each generator and throwing out cancellations and redundancies. If the  $B_i$  are obtained in this fashion, then it suffices to know the number of polyhedra in each  $B_i$  in order to determine the growth function of the group  $G$ .

At the first layer  $B_1$ , new polyhedra are in one to one correspondence with the finite faces on the boundary of  $B_0$ . This is not always the case. On the boundary of  $B_i$ , call a finite face an exposed face if the polyhedron in  $B_{i+1}$  which attaches to that face touches no other polyhedron in  $B_i$  (or  $B_{i+1}$ ) along a face. A finite face is called an edge face if the polyhedron which glues to it attaches by one other adjacent face. This is forced when one of the edges of the attaching face already has three polyhedra meeting it.



A finite face is called a vertex face if the polyhedron which glues to it attaches by two other faces. The three attaching faces must have a common vertex. Here are some pictures:

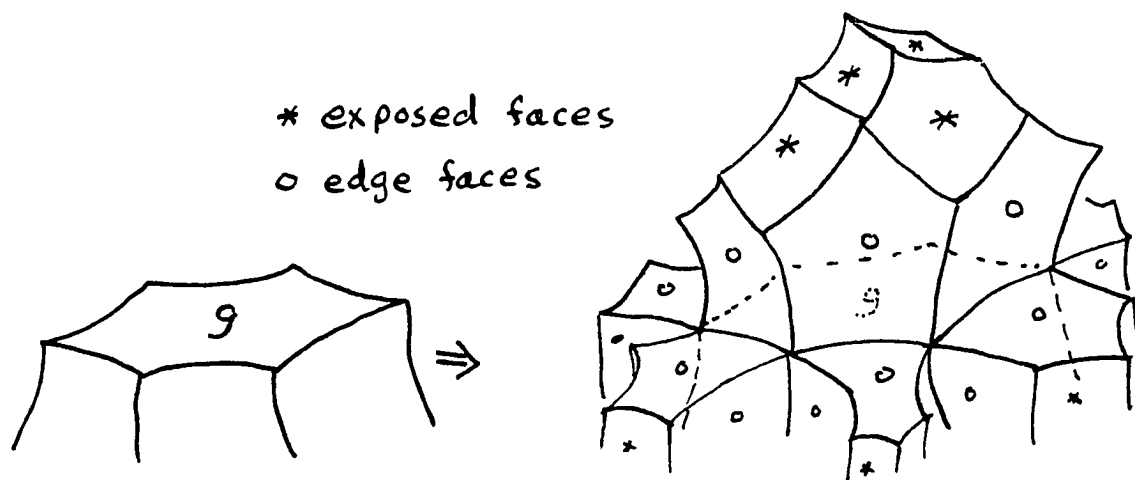
edge faces

vertex  
faces  
 $f, g, h.$ 

We will see that there are no other types of attaching faces.

Here is another characterization. Let  $f$  be a finite face of the boundary of  $B_i$ . If  $f$  is disjoint from  $B_{i-1}$ , then  $f$  is an exposed face. If  $f$  intersects  $B_{i-1}$  along an edge, but is disjoint from  $B_{i-2}$ , then  $f$  is an edge face. If  $f$  intersects  $B_{i-2}$  at a vertex, then  $f$  is a vertex face.

As  $B_0$  has only exposed faces, we start with those. One important property of exposed faces which we must show is that every face adjacent to an exposed face is also on the boundary. This is initially true, and we will see that it is maintained. Suppose that  $P \in B_{i+1}$  is attached to an exposed face  $g$  of  $B_i$  along face  $f = p_g(g)$ . Every face of  $P$  except  $f$  is on the boundary of  $B_{i+1}$ . Faces adjacent to  $f$  meet  $B_i$  along an edge and are hence edge faces.

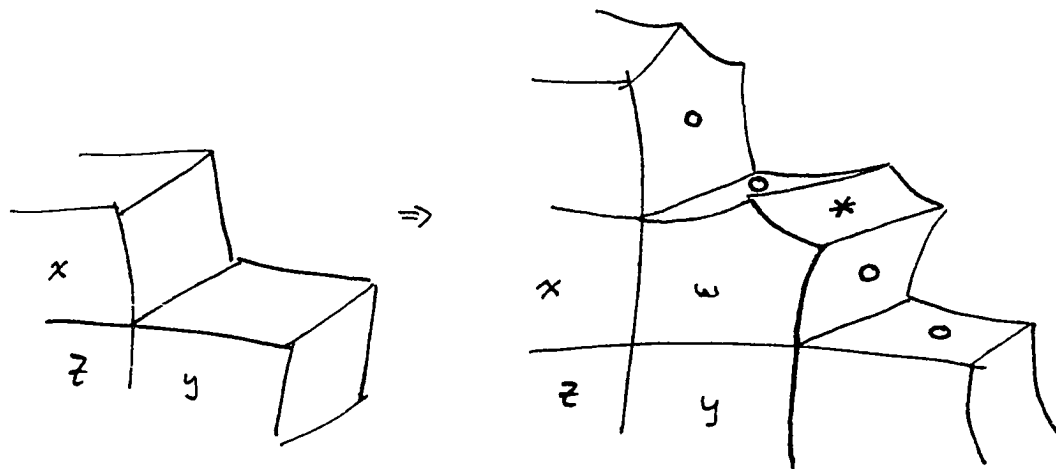


Since  $g$  was an exposed face, the faces adjacent to  $g$  were on the boundary of  $B_i$ , and hence polyhedra in  $B_{i+1}$  were attached along those faces. Thus the picture at each edge,  $e$ , of  $g$  is that of three polyhe-

dra, one from  $B_i$ , two from  $B_{i+1}$ , meeting at  $e$ . When it is time to glue in a polyhedron from  $B_{i+2}$ , it will have to attach to both of the faces on the boundary of  $B_{i+1}$  which meet at edge  $e$ , as we can have only four polyhedra meeting at an edge. The equivalence of the two characterizations of edge faces above follows.

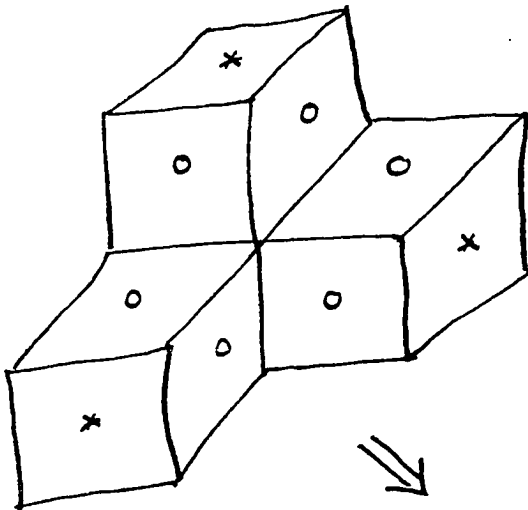
To summarize, if a polyhedron,  $P_j$ , is added along an exposed face,  $f$ , then  $f$  is the only face of  $P_j$  which is not on the new boundary, finite faces of  $P_j$  not touching  $f$  are exposed faces, and finite faces of  $P_j$  adjacent to  $f$  are edge faces. Two edge faces on  $P_j$  intersect iff they have a finite vertex in common with  $f$ . In particular, each edge face can touch no more than two other edge faces of  $P_j$ .

Now suppose that  $P$  in  $B_{i+1}$  is glued to  $B_i$  along a pair  $f$  and  $g$  of faces with common edge  $e$ . First suppose that  $e$  has no finite vertices. This implies that no finite face of  $P$  adjoins both  $f$  and  $g$ . For a finite face of  $P$  which adjoins  $f$  or  $g$ , then, the local picture is that of an edge face. For a finite face of  $P$  not adjoining  $f$  or  $g$ , the local picture is again that of an exposed face.

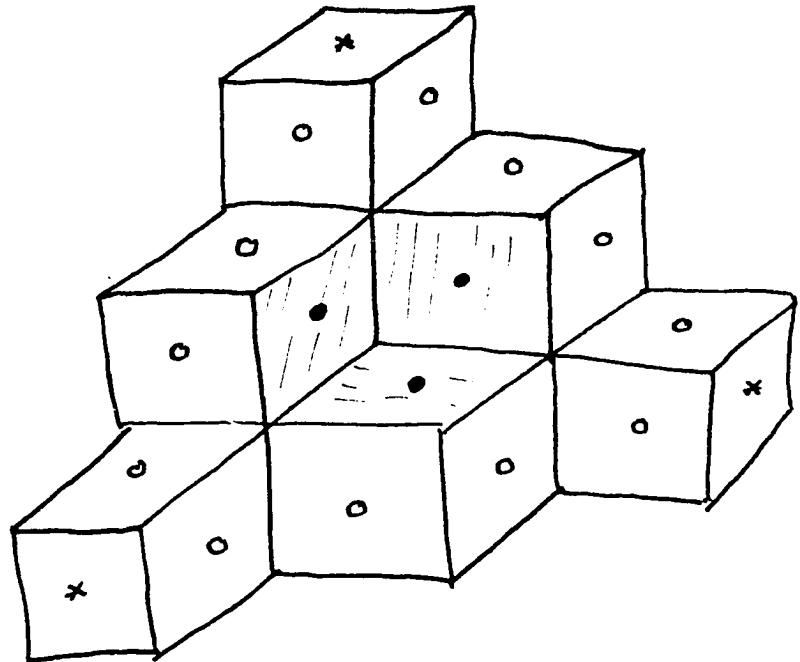


$x, y, z, w$  infinite

If the edge  $e$  of a pair of edge faces does have a finite vertex, then there is a finite face  $h$  of  $P$  which adjoins both  $f$  and  $g$ . What happens to a cell in  $B_{i+2}$  which is attached to  $h$ ? Consider: we have a finite vertex  $v$ . Therefore, three finite edges of  $B_{i-1}$  meet at  $v$ . In  $B_i$ , these are edges of edge faces, and to each pair of edge faces, there is the third face in  $B_{i+1}$  adjacent to both. The copy of  $P$  in  $B_{i+2}$  must glue to all three of these faces, since we must have eight polyhedra and six edges meeting at a vertex.

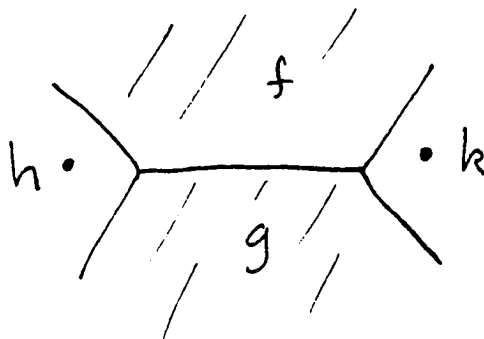


• vertex faces.



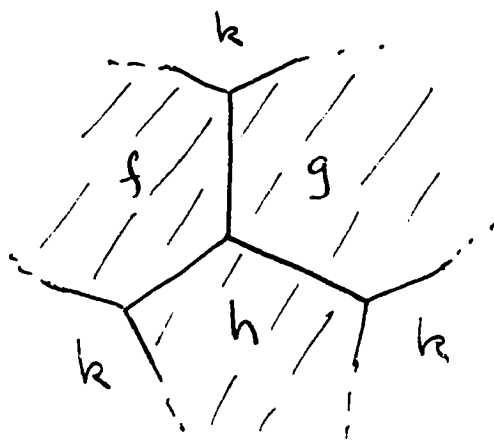
We call these faces vertex faces.

We summarize: If  $P$  is attached along a pair of edge faces, then finite faces which are disjoint from the attaching faces are exposed faces. Finite faces which touch only one attaching face are themselves edge faces. And, if the common edge  $e$  has any finite vertices, we will have vertex faces which adjoin both edge faces. In the event that there are two vertex faces on  $P$ , they must be disjoint. If they intersected, they would have to meet along an edge. But look:



The two 3-cycles of faces  $h$ - $f$ - $k$  and  $h$ - $g$ - $k$  must both have common vertices, and these must be the endpoints of the edge of intersection between  $h$  and  $k$ . But since  $f$  and  $k$  meet along an edge, the common vertex of  $h$ - $f$ - $k$  must be at the other end of that edge. A similar picture holds for the other three pairs. We conclude that the edge of intersection of  $f$  and  $h$  must intersect the edge common to  $f$  and  $k$ . This makes  $f$  a triangle, contradicting the criteria for  $P$ .

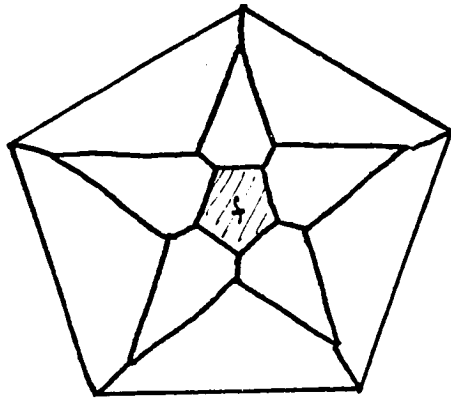
What happens when we attach a copy of  $P$  to a triple of vertex faces? Again, we get three cases. Finite faces disjoint from the attaching faces are exposed faces. Finite faces which adjoin one of the attaching faces are edge faces. Finite faces which adjoin two of the attaching faces are vertex faces. There are no other cases. Why can't a face touch all three attaching faces? Consider this picture:



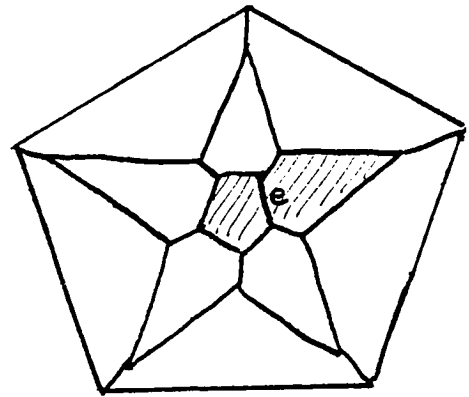
If a face  $k$  adjoined  $f$ ,  $g$ , and  $h$ , then each of the 3-cycles  $f$ - $g$ - $k$ ,  $f$ - $h$ - $k$  and  $g$ - $h$ - $k$  would have a common vertex. In each case, the vertex would have to be the other endpoints of the edges meeting at  $v$ . But since  $k$  can meet  $f$ ,  $g$  and  $h$  at only one edge each, we conclude that  $f$ ,  $g$ ,  $h$ , and  $k$  form a tetrahedron.

Now we make an important observation. The number and types of exposed, edge and vertex faces which appear when a copy of  $P$  is attached to  $B_i$  depends only on the attaching faces and not on  $i$ . Because of this, we can count the number of polyhedra in each layer recursively.

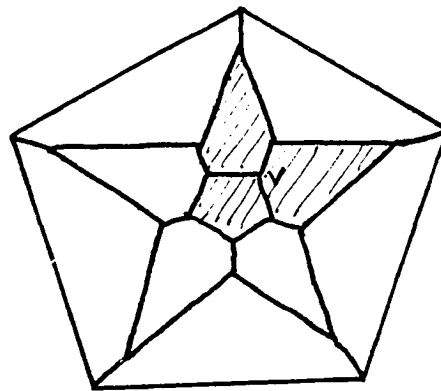
Label each finite face of  $P$   $f_1, \dots, f_n$ . Label each finite edge  $e_1, \dots, e_k$ . Label each finite vertex  $v_1, \dots, v_l$ . To each polyhedron, label it according to how it was attached to the previous layer, e.g., label it  $f_3$  if it was attached to an exposed face along  $f_3$ , label it  $e_7$  if it was attached along two edge faces which intersect along  $e_7$ .



A DODECAHEDRON LABELLED  $f$



$e$



$v$

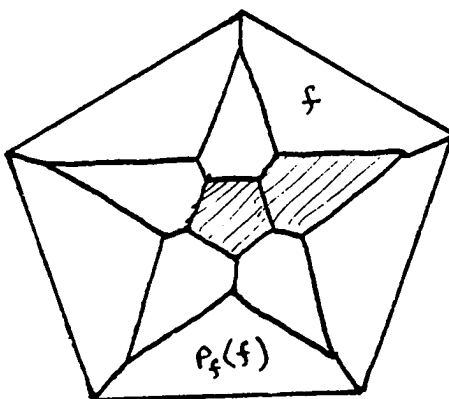
Each new layer of polyhedra determines a vector in the  $n+k+1$  dimensional vector space spanned by the  $f$ 's,  $e$ 's, and  $v$ 's.

There is a matrix  $M$  which relates the vectors of succeeding layers. If  $W_i$  is the vector corresponding to the  $i$ th layer, then

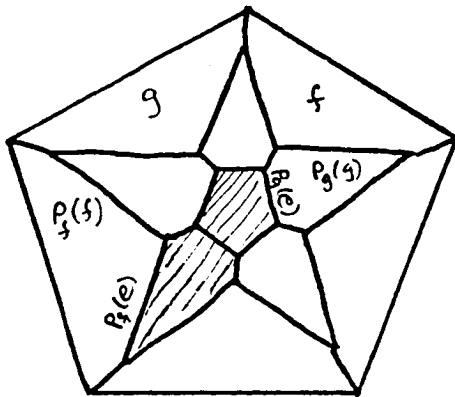
$$W_{i+1} = (M)W_i$$

The coefficients of  $M$  are either 0, 1,  $1/2$ ,  $1/3$ , or  $2/3$ .

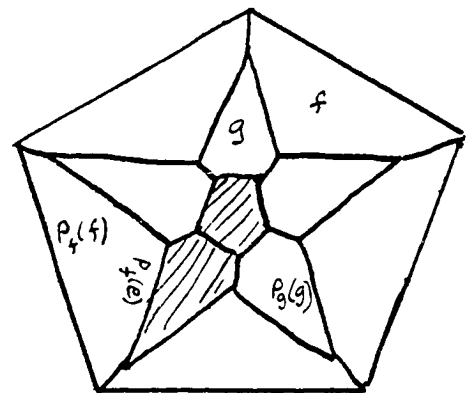
We want to know how many polyhedra in layer  $i+1$  will be attached only along face  $f$ . This is the same as knowing how many exposed faces  $p_f(f)$  lie on the boundary of layer  $i$ . Consider a polyhedron  $P_j$  in layer  $i$ . It was attached along some set of faces. If the face  $p_f(f)$  is disjoint from the set of attaching faces, then it will be an exposed face in the next layer. Therefore, in the column corresponding to  $P_j$  and in the row corresponding to  $f$ , there will be a 1 in the matrix  $M$ .



Consider an edge  $e$ , with adjacent faces  $f$  and  $g$ . There are two faces  $p_f(f)$  and  $p_g(g)$  with distinguished edges  $p_f(e)$  and  $p_g(e)$ . If a polyhedron  $P_j$  is attached along a set  $s$  of faces, then it contributes a  $1/2$  to the row of  $e$  if  $p_f(f)$  intersects the set  $s$  only along the edge  $p_f(e)$ , or the same for  $p_g(g)$ . Actually, if both faces intersect  $s$  properly, then  $P_j$  contributes a full 1 to the row of  $e$ .



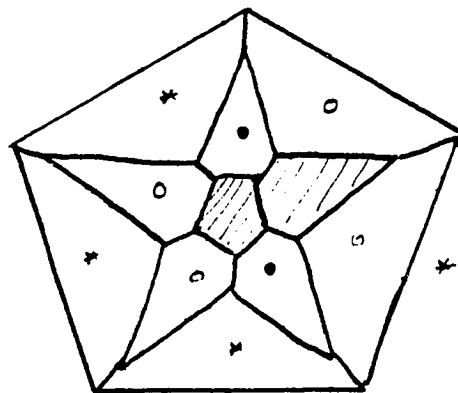
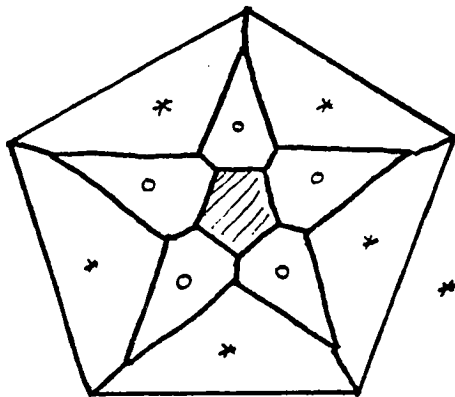
CONTRIBUTES 1, AS BOTH  
 $P_f(f)$  AND  $P_g(g)$  ARE  
 PROPERLY PLACED.



CONTRIBUTES  $1/2$   
 $P_g(g)$  INTERSECTS  
 ALONG 2 EDGES.

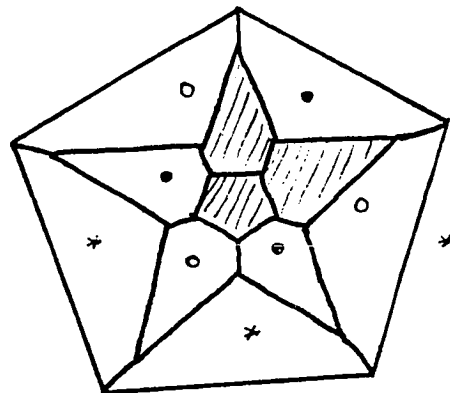
In the case of a vertex  $v$ , look at the adjoining faces  $f$   $g$  and  $h$ . There are three faces with distinguished vertices given by  $(p_f(f), p_f(v))$ ,  $(p_g(g), p_g(v))$ , and  $(p_h(h), p_h(v))$ .  $P$  contributes  $1/3$  to the row of  $v$  for each of these three faces which intersects the attaching set of faces along two edges meeting at the distinguished vertex.

Here are some examples:



The dodecahedron: By symmetry we may group all exposed, edge, and vertex types. The matrix is then

$$\begin{pmatrix} 6 & 4 & 3 \\ 5/2 & 2 & 3/2 \\ 0 & 2/3 & 1 \end{pmatrix}$$



## 2.1 THE MAIN THEOREM

Let  $P$  be a polyhedron with face pairings as in the last section. Suppose that

$$n = \#(\text{finite faces of } P),$$

$$e = \#(\text{finite edges of } P),$$

$$v = \#(\text{finite vertices of } P),$$

$$\chi_{\infty} = (\text{Euler characteristic of the infinite cells}),$$

so that

$$(n - e + v + \chi_{\infty}) = 2,$$

then the group corresponding to  $P$  with face pairings has generating function:

$$\frac{(1+s)^3}{1 + (3-n)s + (\chi_{\infty} - n + v + 1)s^2 + (\chi_{\infty} - 1)s^3}$$

Note: The formula is independent of the choice of face pairings. It depends only on the choice of finite cells. The proof proceeds by finding eigenvectors for the matrix  $M$ . Writing the initial conditions of one copy of  $P$  as a linear combination of the eigenvectors will provide enough information to verify the main assertion.

## 2.2 THE TECHNICAL LEMMA

Let  $P$  be given as above. We make some definitions. Let  $f$  be a finite face of  $P$  and let  $e$  be an edge of  $P$ . Then we define:

$s_f^F$  = the number of finite edges of  $f$  .

$s_f^\infty$  = the number of infinite edges of  $f$  .

$v_f^F$  = the number of finite vertices of  $f$ .

$v_e^F$  = the number of finite vertices of  $e$ .

### 2.2.1 Lemma

If  $\lambda$  is a root of  $\lambda^3 + (3-n)\lambda^2 + (\chi_\infty + v + 1 - n)\lambda + (\chi_\infty - 1) = 0$ , then  $M$  has an eigenvector  $V$  with eigenvalue  $\lambda$  . In particular, the eigenvector  $V$  has coefficients:

$$\lambda^2 + (2 - s_f^F)\lambda - (1 - s_f^\infty)$$

for the face  $f$ ,

$$\lambda - v_e^F + 1$$

for the edge  $e$ , and

$$1$$

for a vertex.

Example: The Truncated Octahedron with Infinite Squares. For each hexagon,  $s_f^F = 3$ , and  $s_f^\infty = 3$ . Each edge is infinite and there are no finite vertices, so since  $n = 8$ ,  $v = 0$  and  $\chi_\infty = 6$ ,  $V$  has coefficients:

$$\lambda^2 - \lambda - 2 \text{ face}$$

$$\lambda + 1 \text{ edge}$$

$$1 \text{ vertex .}$$

Where  $\lambda$  is a root of  $\lambda^3 - 5\lambda^2 - \lambda + 5 = 0$ .

Example: Dodecahedron

$s_f^F = 5$ ,  $s_f^\infty = 0$ ,  $n = 12$ ,  $x^\infty = 0$ , and all edges are finite, so  $V =$

$\lambda^2 - 3\lambda + 1$  face

$\lambda - 1$  edge

1 vertex

Where  $\lambda$  is a root of  $\lambda^3 - 9\lambda^2 + 9\lambda - 1 = 0$

We wish to show that  $MV = \lambda V$ . We first show this for the face coefficients  $V_f$ .

### 2.2.2 The Face Coefficient

$MV$  for the face  $f$  is

$$(MV)_f = \lambda^3 + (2 - s_f^F)\lambda^2 + (1 - s_f^\infty)\lambda,$$

or, using the defining equation for  $\lambda$ ,

$$(MV)_f = (n - s_f^F - 1)\lambda^2 + (n - x_\infty - s_f^\infty - v)\lambda + (1 - x_\infty).$$

How many polyhedra will be attached in the next layer along  $f$ ? The answer is the number of polyhedra which were attached along sets of faces disjoint from  $p_f(f) = g$ . Remember,  $f$  and  $g$  are isomorphic, in particular, they have the same numbers of finite and infinite edges and vertices.

Since the numbers of each type of cell is given by the vector  $V$ , we may compute:

Let  $g^*$  be the union of all finite faces touching  $g$ . Then we have

$$(MV)_f = \sum_{\substack{h \notin g^* \\ h \text{ a face}}} \lambda^2 + (2 - s_h^F) \lambda + (1 - s_h^\infty) + \sum_{\substack{e \notin g^* \\ e \text{ an edge}}} (\lambda - v_e^F + 1) + \sum_{\substack{v \notin g^* \\ v \text{ a vertex}}} 1$$

Call these the face edge and vertex sums.

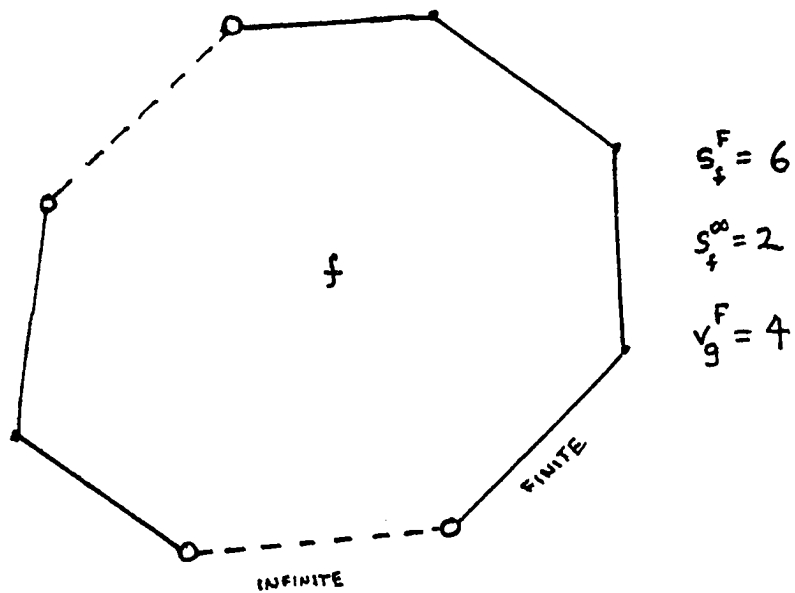
The face sum: The sum over all faces not adjoining  $g$  can be written as the sum over all finite faces of  $P$  minus the sum over the faces in  $g^*$ . Call these sums  $A$  and  $B$ .

$$\text{sum } A = n\lambda^2 + 2n\lambda - 2e\lambda + n - \sum_h s_h^\infty$$

Now we need a formula relating  $s_g^F$  and  $s_g^\infty$ . It is

$$s_g^\infty = s_g^F - v_g^F.$$

This is because at most one infinite edge appears between two finite edges.



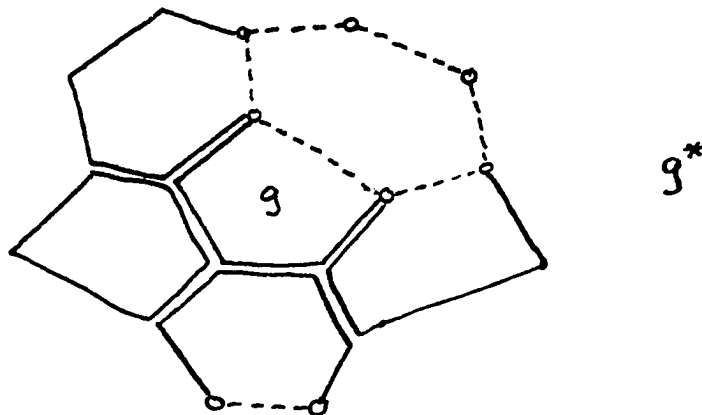
So the last term in sum A is equal to  $2e-3v$ .

$$\text{sum B} = (s_g^F + 1)\lambda^2 + 2(s_g^F + 1)\lambda + (s_g^F + 1) - \sum_{h \in g^*} s_h^F \lambda^{s_h^\infty}$$

Notice that  $\#(f^*) = \#(g^*) = s_f^F + 1$ .

Now look at  $\sum_{h \in g^*} s_h^F \lambda$ .

That counts each edge of  $g^*$  which contains a vertex of  $g$  twice, and every other edge once.



so

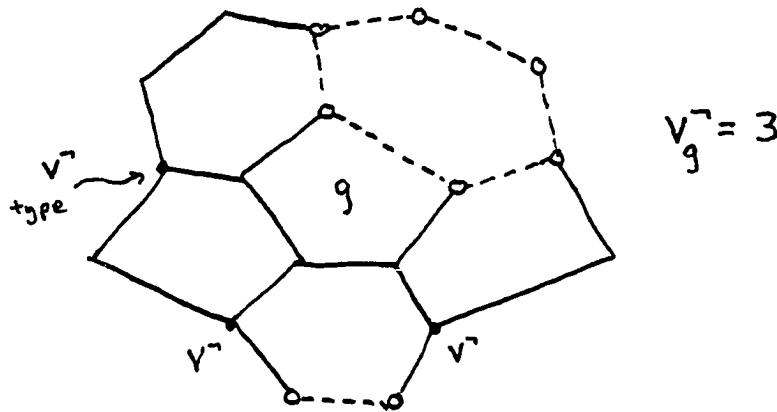
$$\sum_{h \in g^*} s_h^F = e_g^* + s_g^F + (s_g^F - s_g^\infty)$$

Where  $e_g^*$  is the number of finite edges in  $g^*$ . The last term comes from the number of finite vertices of  $f$ .

Similarly,

$$\sum_{h \in g^*} s_h^\infty = \sum_{h \in g^*} (s_h^F - v_h^F)$$

The sum over  $h$  in  $g^*$  of  $v_h^F$  counts each vertex of  $g$  three times, each vertex on the other end of an edge meeting  $g$  twice, (let  $v_g^-$  represent the number of such vertices), and every other finite vertex once.



So sum B =

$$(s_g^F + 1)\lambda^2 + (2 - e_g^* + s_g^\infty)\lambda + (1 - e_g^* + 2v_g^* + v_g^- + v_g^F)$$

Where  $v_g^*$  is the number of finite vertices in  $g^*$ .

Now for the Edge sum. It, too, can be broken up into two sums:

$$\sum_e (\lambda - v_e^F + 1) - \sum_{e \in g^*} (\lambda - v_e^F + 1)$$



Now for the Vertex sum. Adding it up, we get:

$$v - v_g^*$$

So the grand total (after simplification) is:

$$(n - s_g^F - 1)\lambda^2 + (2n - e - 2 - s_g^\infty)\lambda + (n - e + v - 1)$$

But since

$$n - e + v + \chi_\infty = 2,$$

and

$$s_g^F = s_f^F \text{ and } s_g^\infty = s_f^\infty,$$

we have the desired result for faces.

### 2.2.3 The Edge Coefficient

We want

$$(MV)_e = \lambda V_e = \lambda^2 + (1 - v_e^F)\lambda$$

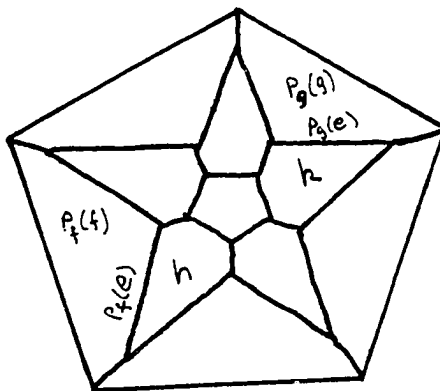
Every polyhedron which contributes to a pair of edge faces has a half share in the polyhedron in the next layer which is attached to that pair. So it is simpler to compute twice the coefficient of  $(MV)_e$ .

We need some definitions. Let

$e^*$  = the pair of faces adjoining  $e$ ,

$e^-$  = the set of edges touching  $e$ .

Let  $f$  and  $g$  be the two faces which adjoin  $e$ . Then there are faces  $h$  and  $k$  such that whenever a polyhedron,  $P$ , in  $B_i$  is attached along  $h$  or  $k$ , there will be a polyhedron,  $Q$ , in  $B_{i+1}$  attached along both  $f$  and  $g$ , that is, along the edge  $e$ . The faces  $h$  and  $k$  are the faces adjacent to the two faces  $p_f(f)$  and  $p_g(g)$  along the edges  $p_f(e)$  and  $p_g(e)$ .



In fact, it is only important that the set of attaching faces of  $P$  contain  $h$  or  $k$  in such a way that the edges  $p_f(e)$  and  $p_g(e)$  intersect no other attaching face.

So  $2(MV)_e =$

$$\sum_{f \in e^*} \lambda^2 + (2 - s_f^F) \lambda + (1 - s_f^\infty)$$

$$+ \sum_{e_j \in e^*} \lambda - e_j^F + 1$$

$$\sum_{v \in e^*} 1$$

Here again, we have face edge and vertex sums. The face sum equals:

$$2\lambda^2 + 4\lambda + 2 - (s_f^F + s_g^F) \lambda - (s_f^\infty + s_g^\infty)$$

The edge sum can be calculated by first summing over each face of  $e^*$  and then subtracting the excess and redundancies.

We get:

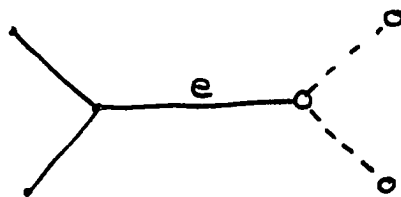
$$(s_f^F + s_g^F)(\lambda + 1) - 2(s_f^\infty + s_g^\infty)$$

$$+ (s_f^\infty + s_g^\infty) - (e^- + 1)(\lambda + 1) + v_e^- + 3v_e^F.$$

And the vertex sum yields:

$$(s_f^F + s_g^F) - (s_f^\infty + s_g^\infty) - v_e^- - v_e^F.$$

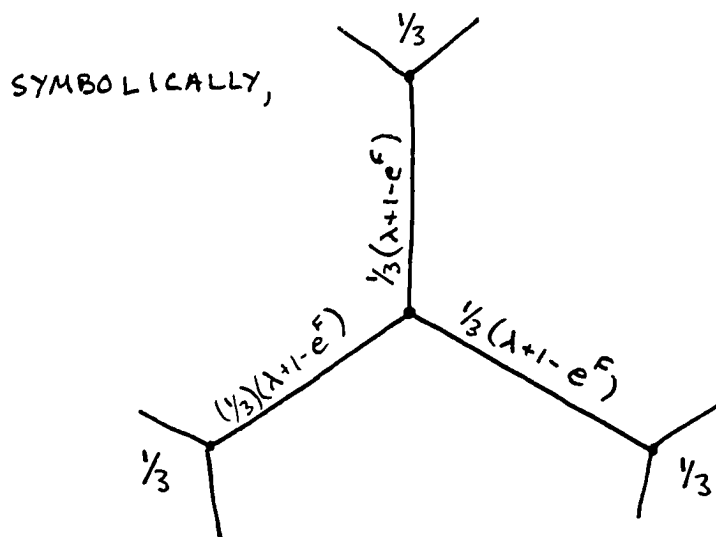
But since  $\#(e^-) = 1 + 2v_e^F$ , we have the desired result when all terms are summed.



$e^- = \text{SOLID LINES.}$

### 2.2.4 The Vertex Coefficient

The case for a vertex is quite simple. A face,  $f$ , on the boundary of  $B_i$  is part of a vertex shaped receptacle iff its polyhedron was attached along a set of faces with two adjacent edges in common with  $f$ . Thus no polyhedron attached along an exposed face can contribute a vertex. Let  $f$ ,  $g$ , and  $h$  be the three faces meeting at a vertex  $v$ . To  $f$ , for example, there are two adjacent faces  $k$  and  $l$  such that  $P$  must be attached along  $k$  and  $l$  for  $f$  to be part of this vertex set of attaching faces. The faces  $k$  and  $l$  are the two faces which adjoin  $p_f(f)$  along the vertex  $p_f(v)$ .



There are thus three edges each of which will contribute  $1/3$  to a new  $v$ , and any finite vertices on any of these edges other than the ones which correspond to  $v$  will also contribute  $1/3$  to a new  $v$ . It is an easy exercise to see that the total contribution will be  $\lambda$ , which is exactly what we want.

### 2.3 THE PROOF OF THE MAIN THEOREM

When we start with our initial polyhedron,  $P$ , the vector representing that state has face coefficients of 1, and all other coefficients 0. Call this vector  $W_1$ . The number of polyhedra in the first layer is just the inner product of  $W_1$  with the vector whose coefficients are all 1. At any layer, we can compute the number of polyhedra by computing:

$$a_n = \langle M^{n-1}W_1, (1, 1, \dots, 1) \rangle$$

Suppose that there were some linear relation among the  $a_i$ , such as:

$$b_n a_k + b_{n-1} a_{k+1} + \dots + b_0 a_{k+n+1} = 0$$

which held for all  $k > N$ . If we took the polynomial

$$q(s) = b_0 + b_1 s + b_2 s^2 + \dots + b_n s^n$$

and the power series

$$(s) = a_0 + a_1 s + a_2 s^2 + \dots + a_i s^i + \dots$$

and took their product, we would get a polynomial:

$$p(s) = p_0 + p_1s + p_2s^2 + \dots + p_{N+n}s^{N+n}$$

Thus we could write:

$$\mathcal{J}(s) = p(s)/q(s)$$

Let  $\lambda_1$ ,  $\lambda_2$ , and  $\lambda_3$  be the roots of the cubic in the Technical Lemma and let  $V_1$ ,  $V_2$ , and  $V_3$  be the associated eigenvectors. We may easily verify, if the eigenvalues are distinct, that:

$$(\lambda_3 - \lambda_1)(\lambda_1 - \lambda_2)(\lambda_3 - \lambda_2)W_1 = (\lambda_1 - \lambda_2)(V_3 - V_1) - (\lambda_3 - \lambda_1)(V_1 - V_2)$$

It follows that the denominator of  $\mathcal{J}(s)$  is as claimed, for the  $W_i$  must satisfy the linear relation defined by the polynomial for the  $\lambda_j$ .

It is a simple, but tedious, exercise to compute the numerator,  $p(s)$ , given the denominator. We know that its degree must be  $\leq 4$ .

It is more of a problem to deal with the case that the eigenvalues are not distinct. If two of the eigenvalues are distinct, say  $\lambda_1 \neq \lambda_2 = \lambda_3$ , then we can observe that:

$$(\lambda_1 - \lambda_2)W_2 = V_1 - V_2 + (\lambda_1 - \lambda_2)\lambda_2 W_1$$

From which it follows that if

$$N = W_1 - V_1/(\lambda_1 - \lambda_2),$$

then

$$(MN) = \lambda_2 N - V_2/(\lambda_1 - \lambda_2)$$

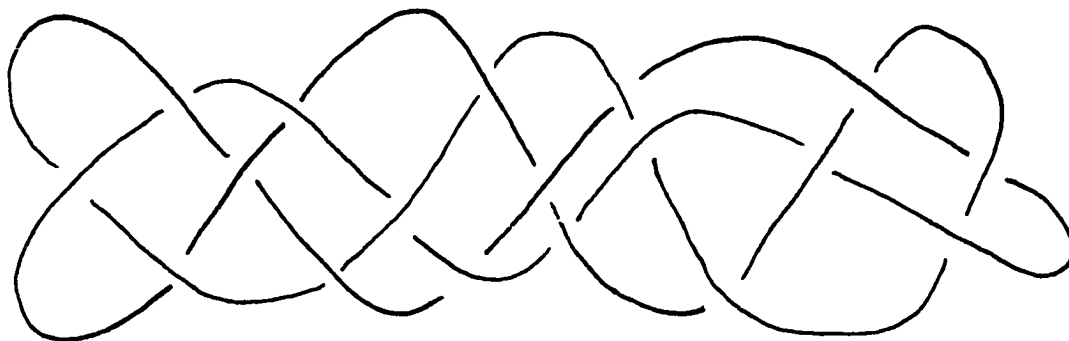
So  $W_1$  is still in the eigenspace of the two eigenvectors.

If all three roots coincide, then the only possible case is the cube, for which the theorem holds. If the root  $\lambda$  were bigger than 1, then consider:

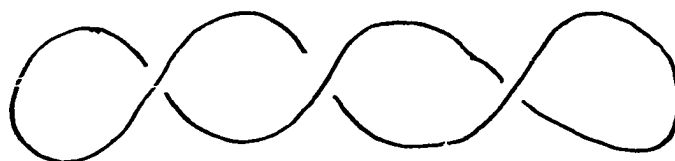
$\chi_\infty = 1 - \lambda^3$ , and  $n = 3 + 3\lambda$ , but then  $v = (\lambda + 1)^3$  (work out the coefficient for the  $\lambda$  term). Now the problem is that  $v \leq 2n - 4$  (equality holds if no faces are infinite). So the only possibility is  $\lambda = 1$ ,  $n = 6$ ,  $v = 12$ ,  $\chi_\infty = 0$ , and the cube is the only admissible polyhedron satisfying these conditions.

## 2.4 THE GROWTH OF ALTERNATING LINK COMPLEMENTS

Let  $k$  be an alternating link in  $S^3$ , that is,  $k$  is a link in  $S^3$  together with a projection to  $S^2$  such that  $k$  alternates between over and under crossings.



Furthermore, suppose that  $k$  is prime in the strong sense that there is no 2-sphere which intersects  $k$  in two places and which separates crossings, and that  $k$  has no trivial twists ( In the cyclic ordering of crossings obtained by following  $k$ , no crossing is hit twice in succession.)



A BAD UNKNOT

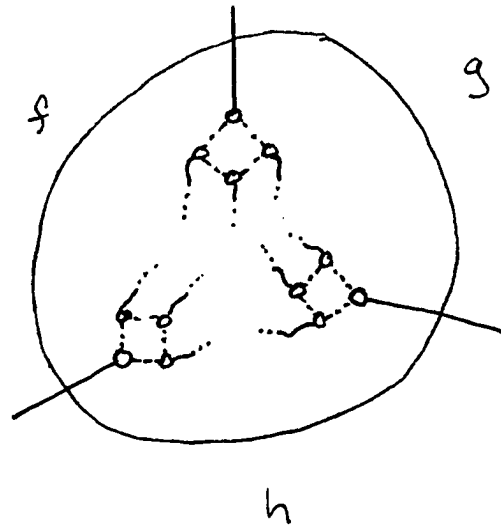
If we now replace the crossings in the projection with tiny infinite squares, we will have an admissible decomposition of the sphere  $S^2$  into faces, edges and vertices.

#### 2.4.1 Theorem

The polyhedron so defined will satisfy the combinatorial properties above.

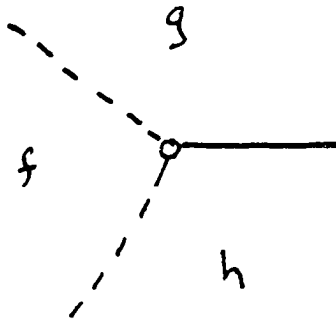
Proof: Conditions 1 - 3 may be verified by inspection. For condition 4, consider: We must show that every 3-cycle of faces has a com-

mon vertex. First, we see that every 3-cycle of faces contains exactly one infinite face. If not, then, back in the 3-sphere, there will be a sphere which crosses the link  $k$  in 3 places.



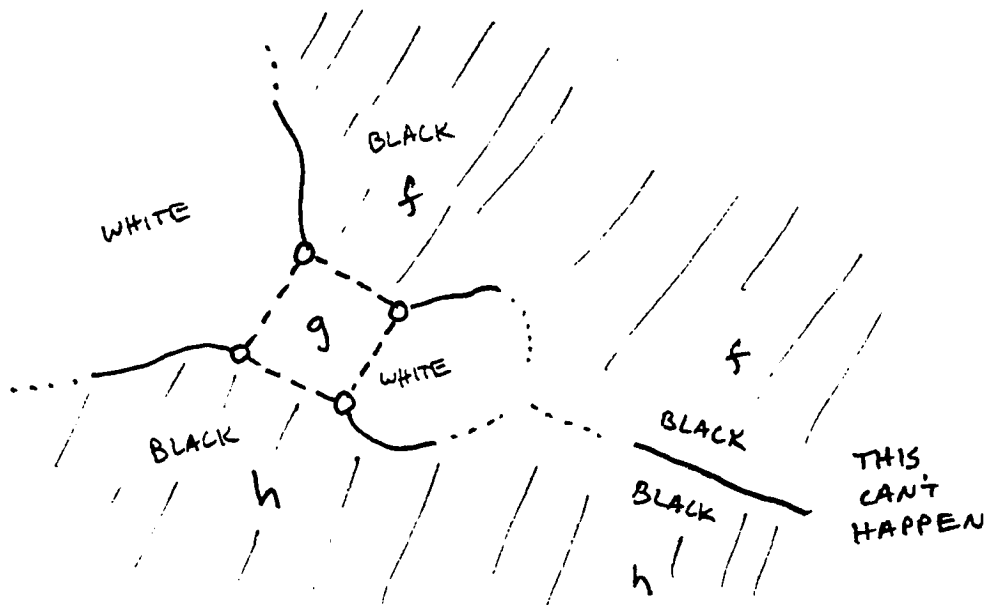
THIS CAN'T  
HAPPEN.

Now, if the cycle passes through one infinite edge, then it passes through two. If the two infinite edges share a vertex, then the 3-cycle contains that vertex.

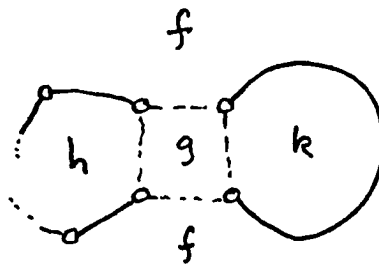


$$(fng) \cap (fnh) \neq \emptyset \\ \Rightarrow (gnh) \neq \emptyset$$

The only remaining case is that the cycle passes through opposite sides of the tiny infinite square. Now the two finite faces involved must intersect along an edge. This is clearly impossible, for one can color the finite faces of  $P$  like a checkerboard, and faces across corners are the same color, but faces which share an edge are opposite colors.



Condition 5 is also clear. The infinite faces are disjoint. If a finite face were to meet an infinite face along two edges, they would have to be opposite edges (coloring again). But then the finite face would meet both of the other two finite faces at that infinite square in two edges.

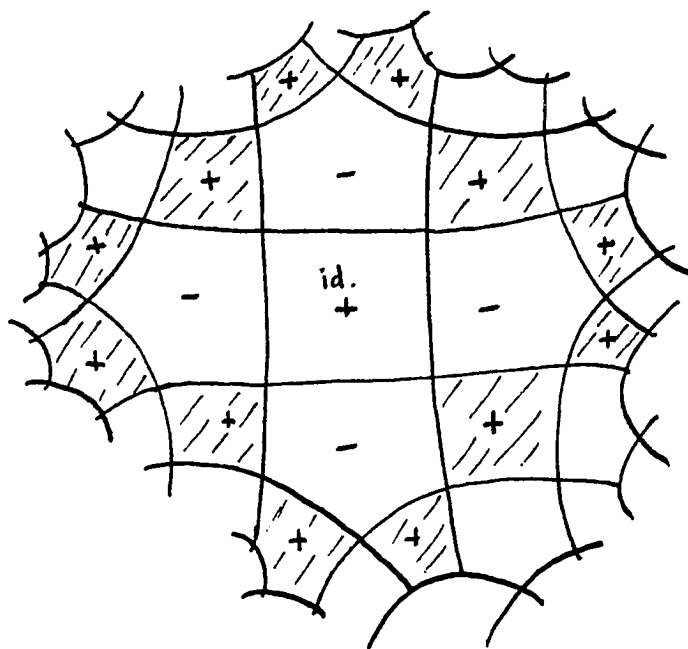


BOTH POSSIBILITIES  
ARE TERRIBLE.  
k HAS 2 EDGES  
(f ∩ h) HAS MORE  
THAN 1 EDGE.

This case is now impossible, for the 2-cycle of finite faces gives rise upstairs to 2-sphere which meets the link in exactly 2 places and which separates crossings.

The face pairings for such a polyhedron were given in an exercise above, but they do not give the link complement. The link complement is made up by two mirror copies of  $P$  which are identified in the pre-

scribed manner. See Menasco [7]. If we think of the 2-sphere in  $S^3$  which defines the crossings of  $k$ , then we can see the two polyhedra, one inside and one outside. If we pick a point inside one as a base point, then we can generate the fundamental group of the link complement by taking paths from the base point into the other polyhedron and back again. In the universal cover, this corresponds to passing across a face of  $P$  into the next layer, and then on to the second. Generators of the fundamental group correspond to polyhedra in the second layer. If we choose the polyhedron with the base point to be positively oriented, then words in the fundamental group are in 1-1 correspondence with the positively oriented copies of  $P$  in the universal cover.



SAMPLE  
CROSSECTION.  
GENERATORS  
SHADED.

Note that the relations at edges are exactly what one would expect from an alternating link.

Since the growth sequence for the fundamental group of the link complement is given by the even numbered terms of the growth function of the group generated by  $P$ , we conclude that the growth function depends only on the number of crossings of  $k$ , that is

#### 2.4.2 Theorem

With  $k$  given as above, we have the growth function of the complement of  $k$  as

$$\frac{1 + 3(n-2)s + (n-3)s^2}{(1-s)(1-(n-3)^2s)}$$

Where  $n = 2 +$  the number of crossings of  $k$ .

This amazing fact was discovered by Jim Cannon one sunny day in May, 1980. I was hooked.

Proof: If we left in the crossings as vertices with four edges meeting at them, then we would have

$$2e = 4v$$

So

$$n = 2 + \#(\text{crossings of } k)$$

For a P of this special form, we have a growth function of

$$\frac{(1+s)^2}{(1-s)(1-(n-3)s)}$$

So the assertion follows by taking the generating function for every other term in this power series.

Chapter III  
SOLV GEOMETRY AND TORUS BUNDLES

Solv geometry is the geometry on  $\mathbb{R}^3$  whose isometries are the solvable Lie group of dimension 3. This group has a nice affine representation as follows:

$$\begin{array}{cccc} e^z & 0 & 0 & x \\ 0 & e^{-z} & 0 & y \\ 0 & 0 & 1 & z \end{array}$$

is the unique isometry taking the origin to the point

$$(x, y, z).$$

The left invariant metric of Solv geometry is determined by the orthonormal co-frame:

$$\theta^1 = e^{-z}dx, \quad \theta^2 = e^z dy, \quad \theta^3 = dz.$$

To get a feeling for Solv geometry, we compute its curvatures and geodesics.

### 3.1 CURVATURE

Our first observation is that the  $(x,z)$  and  $(y,z)$  planes, and any plane parallel to them, are hyperbolic. For example, in the  $(x,z)$  plane, let  $w = e^z$ . Then

$$dw = w dz, \text{ so } \theta^1 = dx/w, \text{ and } \theta^3 = dw/w.$$

which is the metric of the upper half plane. So the sectional curvatures parallel to the  $(x,z)$  and  $(y,z)$  planes is  $-1$ .

We can get the sectional curvature of the  $(x,y)$  plane by a trick. The  $x$  and  $y$  axes are horocycles in their respective hyperbolic planes, but with opposite curvature. It is an easy exercise to see that these are the directions of principal curvature for the  $(x,y)$  plane. Since an  $\mathbb{R}^+$  abelian group of isometries acts on the  $(x,y)$  plane, we conclude that its intrinsic curvature is  $0$ . But the extrinsic curvature is  $-1$ , so the sectional curvature of the  $(x,y)$  plane must be  $+1$ , since for curvatures:

$$\text{Intrinsic} = \text{Extrinsic} + \text{Sectional}$$

for any surface in a Riemannian 3-manifold. See Spivak [11], volume 3.

The structure forms and curvature forms are as follows.

$$d\theta^i = -\omega_j^i \wedge \theta^j \quad \text{so } \omega_j^i =$$

$$\begin{array}{ccc} 0 & 0 & -\theta^1 \\ 0 & 0 & \theta^2 \\ \theta^1 & -\theta^2 & 0 \end{array}$$

$$d\omega_j^i = -\omega_k^i \wedge \omega_j^k + \Omega_j^i \quad \text{so } \Omega_j^i =$$

$$\begin{array}{ccc} 0 & \theta^1 \wedge \theta^2 & -\theta^1 \wedge \theta^3 \\ \theta^2 \wedge \theta^1 & 0 & -\theta^2 \wedge \theta^3 \\ -\theta^3 \wedge \theta^1 & -\theta^3 \wedge \theta^2 & 0 \end{array}$$

So we were right about the sectional curvatures.

### 3.2 GEODESICS

Consider the tangent vectors to a geodesic. With respect to the fixed frame dual to the orthonormal co-frame, these tangent vectors evolve with time. Since all isometries preserve both the frame and the geodesics, we know that this evolution depends only on the coordinates of the tangent vector and not on its location in space. This implies that there is a flow on the unit sphere which defines the evolution of the tangent vector to a geodesic. This can be computed for a tangent vector given its coordinates with respect to the fixed frame.

To compute this vector field, consider: Parallel translation along a geodesic preserves the tangent vector field, but not necessarily an arbitrary vector field. Consider a vector field which is constant with respect to the fixed frame. The infinitesimal change as we parallel translate this vector field along the geodesic is precisely the covariant derivative of the vector field in the direction tangent to the geodesic. In particular, if we start with the constant vector field whose value at a point is tangent to the geodesic, we find that the parallel translate of this fixed vector field varies as its covariant derivative with respect to itself. We thus conclude that, back in the coordinates of the fixed frame, the auto-parallel vector field tangent to the geodesic is evolving as the negative of the covariant derivative of the constant vector field in that direction with respect to itself. To rephrase, there are two vector fields which are both tangent to a given geodesic at a given point. One is constant with respect to the fixed frame, the other is auto-parallel. Parallel translation fixes one and varies the other by its covariant derivative. So in the coordinates in which the non-parallel field is constant, the other varies by the negative of that covariant derivative.

Let us introduce some notation. Let

$$\mathbf{x} = (x_1, x_2, x_3)$$

be the fixed coordinate system on the tangent space. Then if  $X$  is a constant vector field, and

$$Y(t) = (y_1(t), y_2(t), y_3(t))$$

is the tangent field to a geodesic with

$$Y(0) = X$$

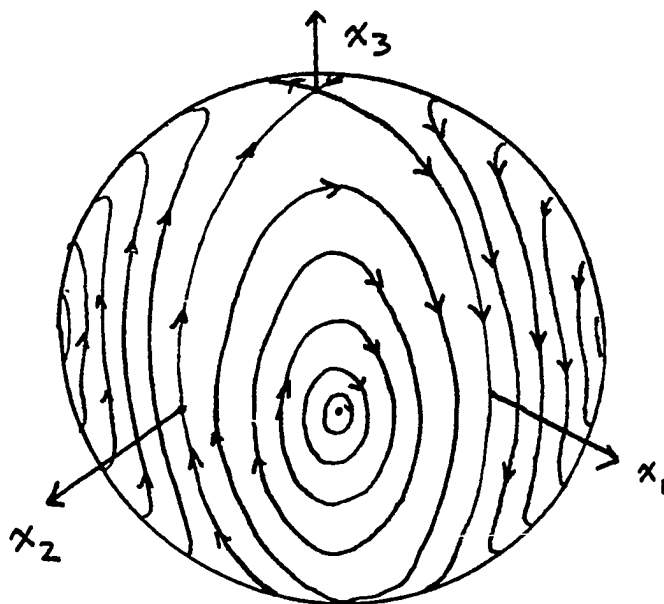
Then

$$Y'(0) = -\nabla_X X$$

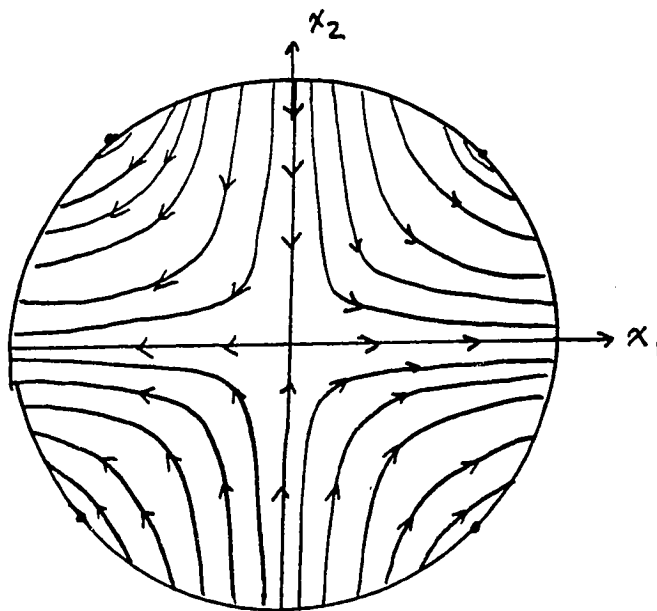
If we compute this vector field using the structure forms for Solv we get:

$$\nabla_X X = (x_1 x_3, -x_2 x_3, x_2^2 - x_1^2)$$

This looks like :



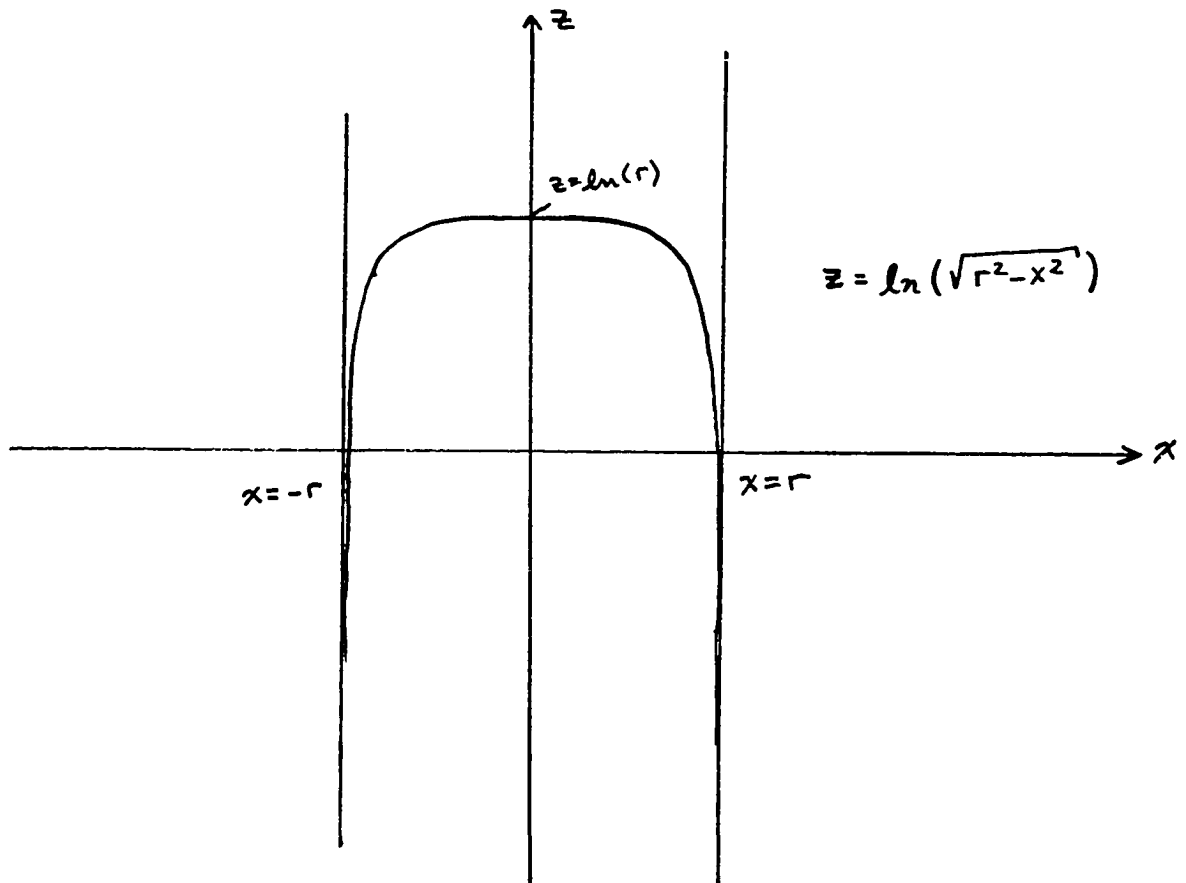
Seen from above, the flow lines are arcs of hyperbolas.

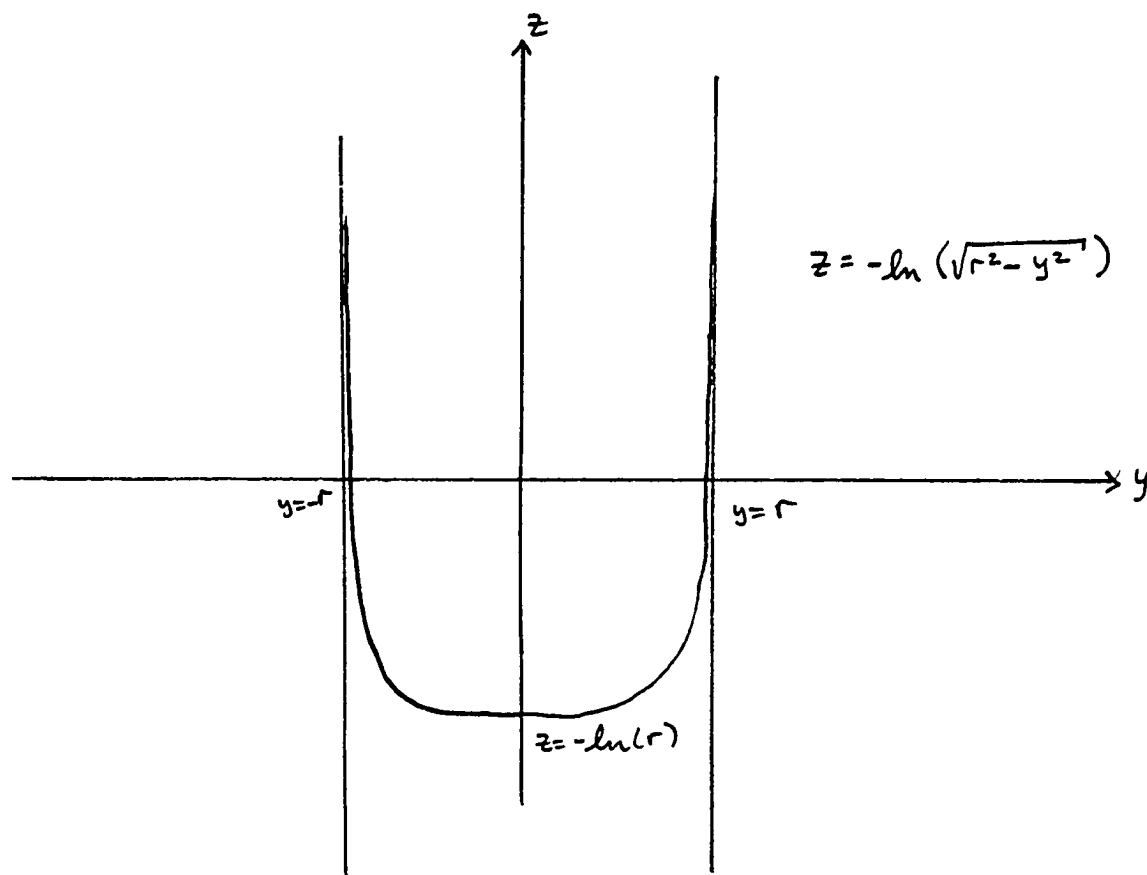


Note that the  $(x,z)$  and  $(y,z)$  planes really are totally geodesic, and that their geodesics behave like hyperbolic lines (a pleasant confirmation). The disturbing fact about this picture is that it indicates that any geodesic not parallel to the  $(x,z)$  or  $(y,z)$  planes spirals about the lines whose tangent vectors are

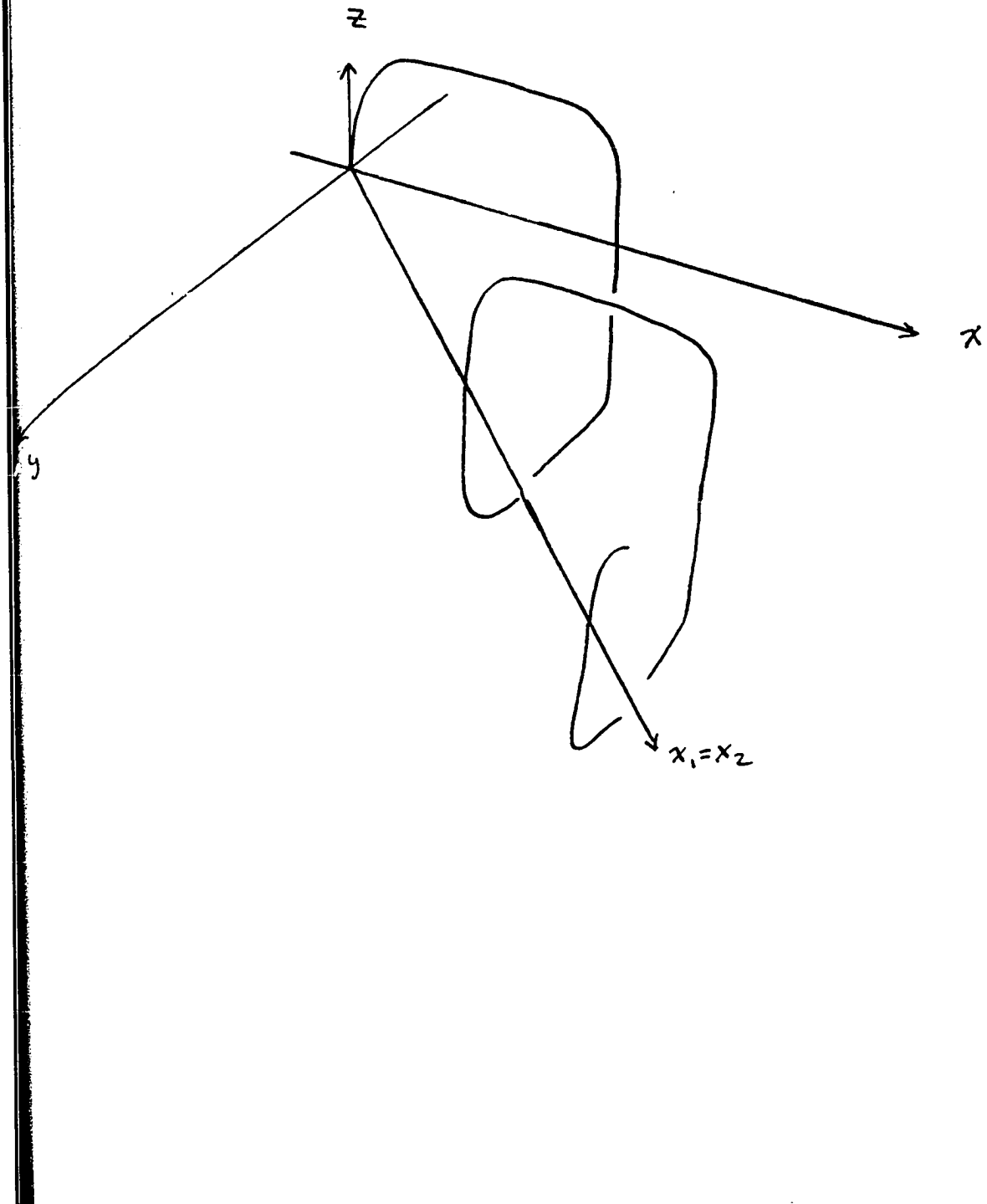
$$(1/2)(\sqrt{2}, \sqrt{2}, 0)$$

To see that this is believable, look again at the geodesics in the two hyperbolic planes. In  $\mathbb{R}^3$ , they look like:

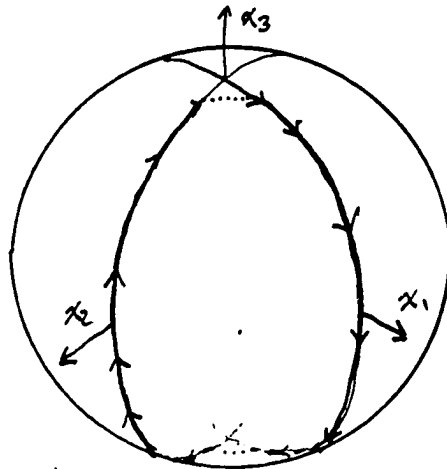




So there is a piecewise geodesic with small exterior angles which looks like this:



On the unit tangent sphere, this path looks like this:



so it closely approximates the orbits close to it.

Now look at the length and travel of this spiral. Take the geodesic in the  $(x,z)$  plane which passes horizontally through the point  $(0,h)$ . By taking  $\exp(\text{vertical scale})$  and looking in the upper half plane, we see that the distance along this geodesic between the points where it hits the  $x$  axis is

$$2\cosh^{-1}(e^d).$$

This is a nice exercise.

Now, back at the piecewise geodesic. One turn of the spiral, assuming height  $d$ , takes less than  $4d+4$  time units, but it reaches the point in the plane

$$(\sqrt{2}e^d, \sqrt{2}e^d)(1-e^{-2d})$$

(Solve for the points where the geodesic above hits the x axis.) But the line

$$(x=y, z=0)$$

is also a geodesic. Look at the fixed points on the unit sphere, or look at the isometry

$$x \leftrightarrow y, z \rightarrow -z.$$

Along this "straight" geodesic, the distance is  $2\sqrt{2}e^d(1-e^{-2d})$ .

Let's get actual expressions for the spiral time and length of travel. Look at the projection of our vector field into the  $(x_1, x_2)$  plane. The flow lines are parameterized by

$$(ae^t, ae^{-t}).$$

Unfortunately, the tangent vectors to these curves are not the same length as the vectors which we wish to integrate. To calculate the period of a spiral, then, we must integrate the ratio of length of the tangent vectors to  $(ae^t, ae^{-t})$  over the length of our vector field  $V$ . We have:

Let  $g_a$  be the geodesic whose tangent vector at the origin is

$$(a, a, \sqrt{1-2a^2})$$

Then the length,  $L(a)$ , of one complete spiral of  $g_a$  is

$$\int_0^{t_0} \frac{4 dt}{\sqrt{1 - 2a^2 \cosh(2t)}}$$

Where  $t_0$  is the value of  $t$  for which the flow line hits the unit circle, or:

$$e^{(2t_0)} + e^{-(2t_0)} = 1$$

Letting  $a$  approach its limiting value of  $(\sqrt{2}/2)$  is interesting, for that yields the lower bound for spiral time, as well as indicating the behaviour of geodesics close to the  $(x_1=x_2, x_3=0)$  lines. The answer is:

$$\pi\sqrt{2}$$

This can be seen by tedious limiting calculations, or by a trick. Go back up to the sphere and project a neighborhood of the fixed point onto the tangent plane to the sphere at that point. In coordinates

$$w = (x_1 - x_2)/\sqrt{2}, \quad x_3$$

The vector field approximates,

$$(-x_3, 2w)$$

which is integrated by

$$(\alpha \cos(\sqrt{2}t), \alpha\sqrt{2} \sin(\sqrt{2}t))$$

so a period of  $\pi\sqrt{2}$  is indicated.

How about the actual shape of the spiral? Well, for large spirals we have a pretty good idea. Let's be exact. With  $a$  and  $t_0$  as before, the  $z$  travel of a geodesic starting at  $t=0$  and going to  $t=t_1$  is

$$\int_0^{t_1} \frac{x_3(t) dt}{\sqrt{1-a^2(e^{2t_1} + e^{-2t})}}$$

Since the integrand evaluates to 1, we have that  $z$  is just piecewise linear in  $t$ .

Now remember that in  $R^3$  there is a distortion of  $e^z$  in the  $x$  direction when we go up by  $z$ , so the  $x$  travel of a geodesic is

$$\int_0^{t_1} \frac{x_1(t) e^{z(t)} dt}{\sqrt{1-a^2(e^{2t}+e^{-2t})}}$$

which is equal to

$$\int_0^{t_1} \frac{ae^{2t} dt}{\sqrt{1-a^2(e^{2t}+e^{-2t})}}$$

Assuming that the geodesic at time  $t=0$  is starting at the steepest part of its spiral (that indicated in all of the pictures), then by symmetry, the distance,  $D(a)$ , along the line  $x=y$ ,  $z=0$  from the origin to the point of first return of the geodesic  $g_a$  is:

$$\int_0^{t_0} \frac{2\sqrt{2}a(e^{2t}+e^{-2t}) dt}{\sqrt{1-a^2(e^{2t}+e^{-2t})}}$$

We can show that the spiral lies on a Euclidean cylinder as follows:

The w coordinate above develops like

$$\frac{1}{\sqrt{2}} \int_0^{t_0} \frac{a(e^{2t}-e^{-2t}) dt}{\sqrt{1-a^2(e^{2t}+e^{-2t})}}$$

So, as  $z=t$ , we have a geodesic on the cylinder:

$$w^2 + \cosh(2z) = (1/2a^2)$$

If we have a geodesic whose tangent vector at the origin is not pointing in the  $x = y$  direction, then we can let it evolve until it does (assuming, of course, that it is not in the  $(x,z)$  or  $(y,z)$  planes). The geodesic will now be at some point  $(a,b,h)$ . Its evolution from this

point onwards will be a translate of the geodesic at the origin with the same tangent vector. That is, it will spiral about the line:

$$(x-a) = e^{2h}(y-b), \quad z = h.$$

To see some of these numbers, here is a computer generated table of some choice spirals, where  $\theta$  is the angle between the tangent vector and the  $(x_1, x_2)$  plane.

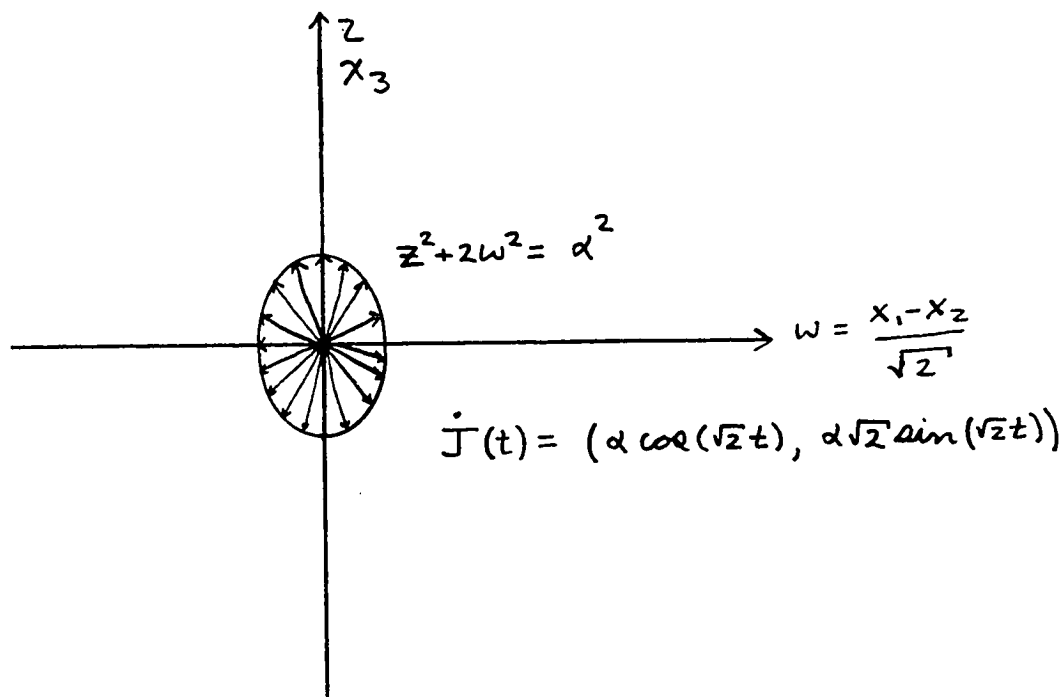
a	$\theta$	L	D	D/cosh(L/4)
0.70786	0.00763	4.4428	4.45788	0.93653
0.70622	0.05007	4.4468	4.54415	0.95385
0.70194	0.12092	4.4672	4.69377	0.98125
0.68265	0.26374	4.5608	5.0230	1.03035
0.64864	0.40951	4.7320	5.4136	1.07211
0.59889	0.56053	5.0120	5.9094	1.10355
0.53134	0.72057	5.4404	6.5987	1.12346
0.44125	0.89690	6.1280	7.7187	1.12680
0.31517	1.10881	7.4200	10.206	1.10168
0.22342	1.24932	8.7760	13.743	1.06994
0.10000	1.42890	11.985	28.991	1.02318
0.07071	1.47063	13.368	40.5675	1.01323
0.03162	1.52606	16.584	89.7632	1.00436
0.01000	1.55663	21.192	282.955	1.00069
0.003126	1.56632	25.796	894.402	1.00057
0.00100	1.56938	30.402	2828.14	1.00030

The shapes of the cylinders for these geodesics are given by their maximum  $w$  and  $z$  coordinates:

$w_{\max}$	$z_{\max}$
0.00763	0.00539
0.05011	0.03542
0.12151	0.08581
0.27003	0.18979
0.43404	0.30229
0.62770	0.43043
0.87808	0.58666
1.25217	0.79798
2.00835	1.14962
3.00277	1.49744
7.00023	2.30256
9.94995	2.64915
22.33831	3.45387
70.7036	4.60517
223.6045	5.75646
707.1060	6.90775

Note that these approach constant multiples of  $D$  and  $L$ .

The computer numbers suggest that the spirals always get where they are going faster than the straight geodesic. We have seen that this is the case for large spirals. We can use the curvature forms for Solv geometry to calculate the Jacobi fields along the straight geodesic. They indicate that the point  $(\pi, \pi, 0)$  is a conjugate point of the origin. You can see this geometrically on the unit tangent sphere. If the Jacobi field takes the straight geodesic to a nearby geodesic, then the difference of their tangent vectors is the derivative of the Jacobi field. But the tangent vector to the straight geodesic is constant, so the derivative of the Jacobi field points from the tangent vector  $(\sqrt{2}, \sqrt{2}, 0)$  to the orbit of the tangent vectors of the nearby geodesic. The integral of this new vector field is zero precisely when the nearby geodesic has made one full orbit, or, in the limit, after a time of  $\pi\sqrt{2}$ .



Let  $\theta$  be the angle that a tangent vector in the  $x_1=x_2$  plane makes with the  $(x_1, x_2)$  plane. Consider the geodesic  $g_\theta$  which passes through the origin with this tangent vector. Let  $L(\theta)$  be the arc length of one full spiral turn of  $g_\theta$ . Let  $D(\theta)$  be the distance from the origin to the point  $g_\theta(L(\theta))$  along the  $x=y, z=0$  geodesic. Then the computer calculations suggest that:

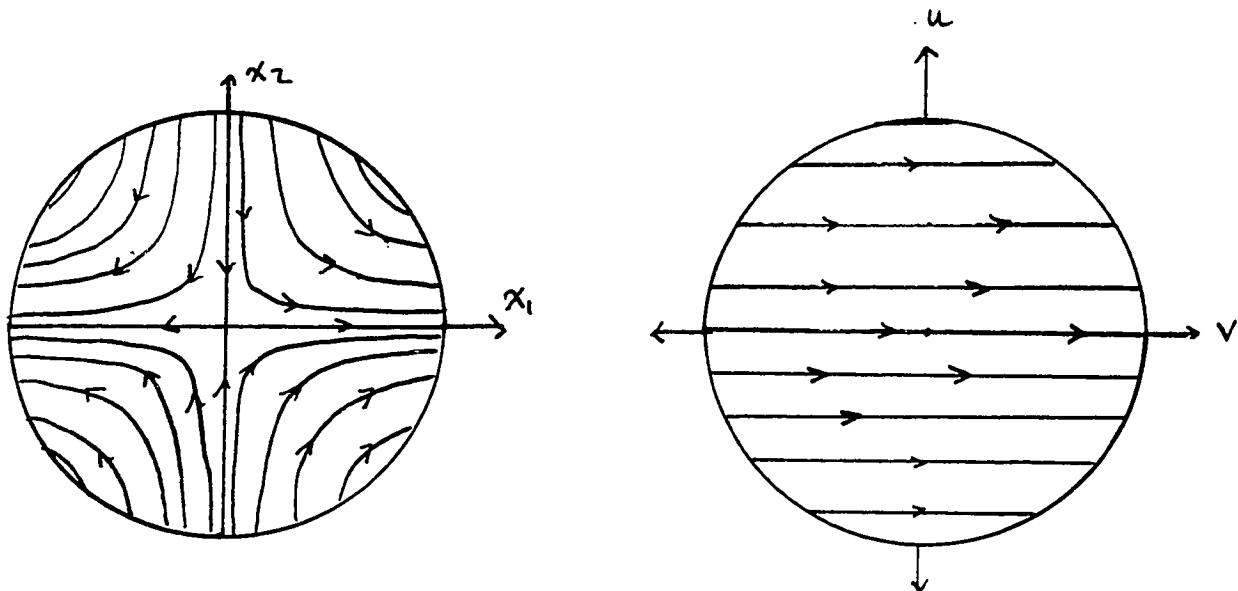
### 3.2.1 Lemma

$L(\theta)$  increases monotonically with  $\theta$ , and

$$D(\theta) > L(\theta) \text{ for } \theta > 0.$$

Note: for large  $D$  and  $L$ , we know that  $D$  approximates  $2\sqrt{2}e^{L/4}$ .

We verify this as follows: The vector field is difficult to deal with in its present form, so we make a change of coordinates which wraps the sphere twice around the  $z$  axis. The actual transformation is given by projecting to the  $(x_1, x_2)$  plane, squaring, in the complex sense, and projecting back orthogonally to the sphere. This change of coordinates sends every orbit of  $V$  to a circle.



In the  $(u, v, w)$  coordinate system, the vector field looks like:

$$(0, 2wN, -2vN)$$

Where  $N$  equals

$$(1/w)\sqrt{(u^2+v^2)}(1-\sqrt{(u^2+v^2)})$$

Since the diameter of an orbit through  $(u,v,w)$  is  $\sqrt{1-u^2}$  we can correct for the size of each orbit to obtain the angular velocity of  $V$ . We obtain:

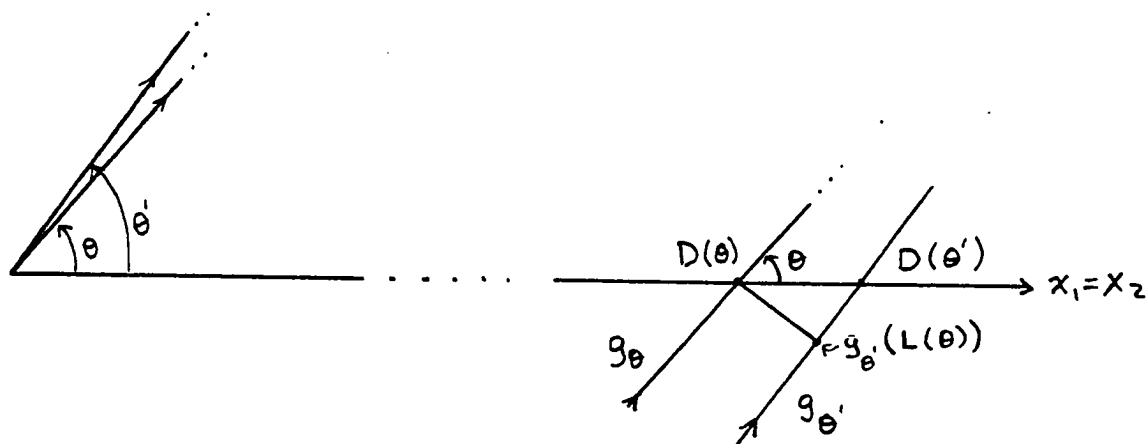
$$|V|_{\text{ang}}^2 = 4N^2$$

Now consider any great circle through the fixed point  $(1,0,0)$  which is not the equator. On this circle,  $v=cw$ , so the angular velocity is simply a function of  $w$ . As  $w$  increases, so does the parameter  $\theta$ , so if the derivative of the angular velocity with respect to  $w$  is negative for all  $c > 0$ , then the orbits with larger  $\theta$  take longer to complete. The derivative of the square of the angular velocity is just

$$(4/w^3)((w^2+2)\sqrt{1-w^2} - 2)$$

which, thank Gauss, is negative for  $w > 0$ . (It even vanishes to the right order.) The assertion follows.

Now consider a geodesic  $g_\theta$  and a nearby geodesic  $g_{\theta'}$  with  $\theta' > \theta$ . Since  $L(\theta')$  is greater than  $L(\theta)$ , we know that at the time  $L(\theta)$ , the larger spiral has not yet completed one full turn. Therefore, the picture at the point of first return is.



That is,  $g_{\theta'}(L(\theta'))$  is further from the origin than  $g_{\theta}(L(\theta))$ . From this picture, we conclude that the derivative of  $D$  with respect to  $L$  is  $\sec(\theta)$ , which is always greater than 1, for  $\theta > 0$ . Since  $D(0) = L(0) = \pi\sqrt{2}$ ,

we conclude that  $D > L$ , as desired. In fact, as  $\theta$  is always increasing with  $L$ , we conclude that the second derivative of  $D$  with respect to  $L$  is always positive, except at 0, where it vanishes. This has the following implication:

### 3.2.2 Theorem

Let  $(p, p, 0)$  be a point on the line  $x=y, z=0$ , with  $p > \pi^2$ . Then the shortest path from the origin to  $(p, p, 0)$  is the spiral  $g_{\theta}$  with  $D(\theta) = \sqrt{2}p$ . There are other geodesics from the origin to  $(p, p, 0)$ , but they are all longer in length. In particular, suppose that for some integer  $k$ ,  $p/k > \pi$ , but  $p/(k+1) \leq \pi$ . Then there are  $\theta_i, 1 \leq i \leq k$  such that

$$\theta_1 > \theta_2 > \dots > \theta_k > 0$$

such that

$$D(\theta_i) = D(\theta_1)/i$$

and the distances from  $(0,0,0)$  to  $(p,p,0)$  along the associated geodesics  $g_{\theta_i}$ , that is,  $iL(\theta_i)$ , increases with  $i$ , and  $kL(\theta_k)$  is less than  $\sqrt{2}p$ .

So there are  $k+1$  different lengths of geodesics from  $(0,0,0)$  to  $(p,p,0)$ , and the geodesics are unique up to isometry ( $g_{\theta}$  is a translate of  $g_{-\theta}$ .)

### 3.3 GEODESICS IN TORUS BUNDLES

In this section we will discuss the closed geodesics in the free homotopy classes of torus bundles over circles with Anosov monodromy. Such manifolds have universal covers modelled on Solv geometry. There are many different Solv geometric structures on a given torus bundle, determined by choosing the modulus and the area of the torus. Given a choice of a structure on the torus bundle, we will see that for a given free homotopy class, there is always a shortest closed geodesic, and there is also often a unique longest closed geodesic. In fact, there are often several, but always a finite number of distinct lengths of closed geodesics representing a given free homotopy class.

#### 3.3.1 The Solv Geometry Structure on Torus Bundles

Let  $M$  be a manifold obtained by taking the product of a torus with a closed interval and identifying the two boundary components by a homeomorphism. As homeomorphisms of the torus to itself are defined up

to isotopy by elements of  $SL_2\mathbb{Z}$ , we may associate to the manifold the matrix which defines its monodromy. If the matrix  $\Psi$  has real distinct eigenvalues, then we say that  $\Psi$  is hyperbolic, and that the homeomorphism induced by  $\Psi$  is Anosov.

### 3.3.2 Theorem

Let  $M$  be a torus bundle with Anosov monodromy. Then  $\pi_1(M)$  acts on Solv Geometry as a discrete cocompact group of isometries.

Proof: See Scott [10]. Since  $\Psi$  is hyperbolic, it has two distinct eigenvectors with real distinct eigenvalues.  $\pi_1(M)$  has a normal  $\mathbb{Z}+\mathbb{Z}$  subgroup corresponding to  $\pi_1(\text{torus})$ . Choose a representation of this subgroup on  $\text{Isom}(\text{Solv})$  in such a way that the eigenvectors are taken to translation along the  $x$  and  $y$  axes. That is, there is a lattice,  $L$ , in the plane which is the image of the integer lattice under a linear map which takes the two eigendirections to the  $x$  and  $y$  axes. Generators for the  $\mathbb{Z}+\mathbb{Z}$  subgroup are represented as generators for the lattice  $L$ . This choice determines the structure uniquely. The remaining generator of the group, which corresponds to the circle direction, is represented as an isometry which takes the origin straight up a height  $\log(\lambda)$ . It is left to the reader to convince herself that this completes the proof. Note: a vertical translation by  $\text{Log}(\lambda)$  expands by a factor of  $\lambda$  in the  $x$  direction and compresses by a factor of  $\lambda$  in the  $y$  direction, which is exactly what  $\Psi$  should do.

We are now ready to find the closed geodesics. Let  $w$  be a word representing an element of  $\pi_1(M)$ . There are two cases.

Case 1:  $w$  sends the origin to the point  $(a,b,h)$ ,  $h \neq 0$ .

Case 2:  $w$  sends the origin to the point  $(a,b,0)$ .

We will first look at Case 1.

### 3.3.3 Proposition

If  $w$  sends the origin to  $(a,b,h)$ ,  $h \neq 0$ , then there is a unique closed geodesic representing the class of  $w$ . Furthermore, the geodesic is the quotient of a vertical line in Solv geometry.

Proof:  $w$  acts on the space of vertical lines by the affine transformation

$$\begin{pmatrix} e^h & 0 & a \\ 0 & e^{-h} & b \end{pmatrix}$$

Where we identify a vertical line by its first two coordinates. This has a unique fixed line which we can solve for as

$$\left( \frac{a}{1-e^h}, \frac{b}{1-e^{-h}} \right)$$

Since  $h \neq 0$ .

To see that no other geodesic can represent  $w$ , remember that not only must  $w$  take one point on the geodesic to another one, but it must also take the tangent vector to the geodesic at the first point to the tangent vector at the second. Examination of the vector field  $V$  on the unit tangent sphere reveals that the only geodesics which point in the same directions at different heights are the vertical geodesics. Since only one vertical line is fixed by  $w$ , we conclude that it represents the unique geodesic in the class of  $w$ .

We now turn to Case 2. Let  $w$  be an element of  $Z+Z$ , that is,  $w$  is represented as a horizontal translation. The action of  $w$  is to take the origin to some point  $(a,b,0)$

Look at all of the images of the line  $z=0, x=y$  under transformations which take the origin to a point on the  $z$ -axis. The line through the point  $(0,0,h)$  is given by

$$z = h, \quad x = e^{2h}y.$$

Call these lines the straight horizontal geodesics.

Since  $\Psi$  is hyperbolic, we conclude that no eigenvector of  $\Psi$  has rational slope. Thus, no image of the origin by a non-trivial element of  $Z+Z$  lies on the  $x$  or  $y$  axes. Therefore, if

$$h = (1/2)\text{Log}(a/b),$$

then the line

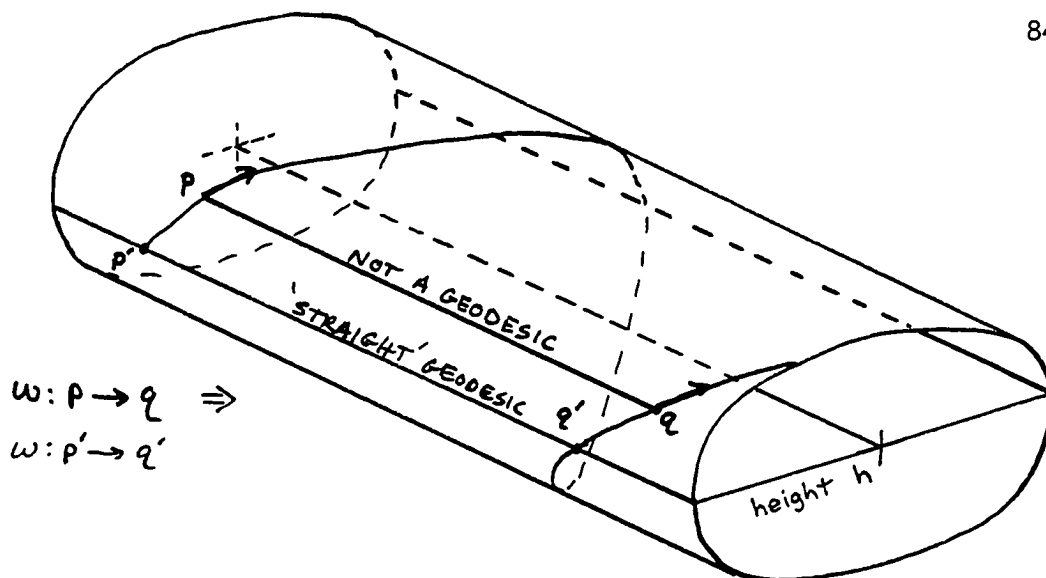
$$z=h, x=(a/b)y,$$

is preserved by the action of  $w$ . We have thus found one geodesic in the free homotopy class of  $w$ . The length of this geodesic is

$$\sqrt{2ab}$$

which is important, for it tells us exactly how many different lengths of closed geodesics lie in the same free homotopy class. The geodesic which we have found, denote by  $g_0$ . If the length of  $g_0$  is greater than  $\pi/2$  then there exists a spiral geodesic which completes exactly one full turn between the point  $(0,0,h)$  and  $(a,b,h)$ . Call this geodesic  $g_1$ . We saw in the last section that there are a number of different length geodesic arcs connecting  $(0,0,0)$  with  $(p,p,0)$  if  $p$  is sufficiently large. By a vertical shift of  $h$ , we get a collection of different length geodesic arcs completeing integral numbers of spirals between  $(0,0,h)$  and  $(a,b,h)$ . These represent the different length closed geodesics in the free homotopy class of  $w$ .

To see that these are the only geodesics in the free homotopy class of  $w$ , consider: If the action of  $w$  preserves the tangent vector of the geodesic, then the geodesic must make an integral number of complete turns between points which are identified by the action of  $w$ . If points  $p$  and  $q$  have a full turn of geodesic arc between them, then there are points  $p'$  and  $q'$  on this geodesic with a full turn between them such that they also lie on a straight geodesic.



Since we have found the only straight horizontal geodesic fixed by  $w$ , it follows that the only closed geodesics in the class of  $w$  are those which spiral at height  $h$ .

We have found the number of different lengths of geodesics in the class of  $w$ , but the geodesics themselves are not so unique. Any horizontal translate of any geodesic in the class of  $w$  will also represent  $w$ . That is, for  $g_0$ , there is an  $S^1$  of translates of  $g_0$  which are all longest geodesics representing  $w$ . For all shorter geodesics, there is a  $T^2 = S^1 \times S^1$  of translates of each. The total picture is this: The space of longest geodesics representing  $w$  is an incompressible torus (the  $(x, y)$  plane /  $Z+Z$ ) foliated by translates of  $g_0$ . About each translate of  $g_0$  is a family of concentric compressible tori, each foliated by translates of closed geodesics of the shorter lengths. Or, if you want, you can find families of incompressible tori (not the  $(x, y)$  plane, but isotop-

ic to it) which are foliated by the closed geodesic of your choice. The pictures are beautiful.

## Chapter IV

### THE GROWTH OF TORUS BUNDLES

We wish to study the growth functions of the fundamental groups of torus bundles over a circle. We start by choosing generators for the fiber  $a$  and  $b$ , which commute, and a generator  $t$  for the circle direction. Before we compute the growth function with these generators, let us look at the limiting case as the monodromy becomes unbounded.

#### 4.1 THE LIMITING CASE

What is the smallest group which has every torus bundle group as a quotient? A first try might be  $(Z+Z)*Z$ . A growth matrix for this group is given by:

$$\begin{array}{ccc} 1 & 0 & 4 \\ 1 & 1 & 0 \\ 2 & 2 & 1 \end{array}$$

Where the columns correspond to exposed types, edge types, and free types. The exact definitions are left as an exercise. In any case, you may verify that the growth function is:

$$\frac{(1 + s)^2}{1 - 4s - s^2}$$

Of course, one can use the formulas for free products of groups to arrive at the same answer, but this is more fun. This has a growth rate of  $2 + \sqrt{5}$ , which is too large. Computer studies indicate a maximum of around  $3 \frac{1}{3}$ . There are, however, a few relations which we can add.

For any finite monodromy  $\Psi$ , the words  $tat^{-1}$  and  $tbt^{-1}$  are words in  $a$  and  $b$ , that is, they commute with  $a$  and  $b$ . If we require this in the limit as well, we get the super-group  $G^\infty$  with generators  $a$ ,  $b$ , and  $t$ , such that  $a$  and  $b$  commute, and both  $a$  and  $b$  commute with the words  $tat^{-1}$  and  $tbt^{-1}$ . Any torus bundle is a quotient of this group. Furthermore, one can see that the growth functions for torus bundles converge in the weak sense to the growth function for the super-group as the coefficients of  $\Psi$  become unbounded.

Here is the important point. The word  $tat^{-1}$  in the super group commutes with  $a$  and  $b$ , but is not equal to any word in  $a$  and  $b$ .

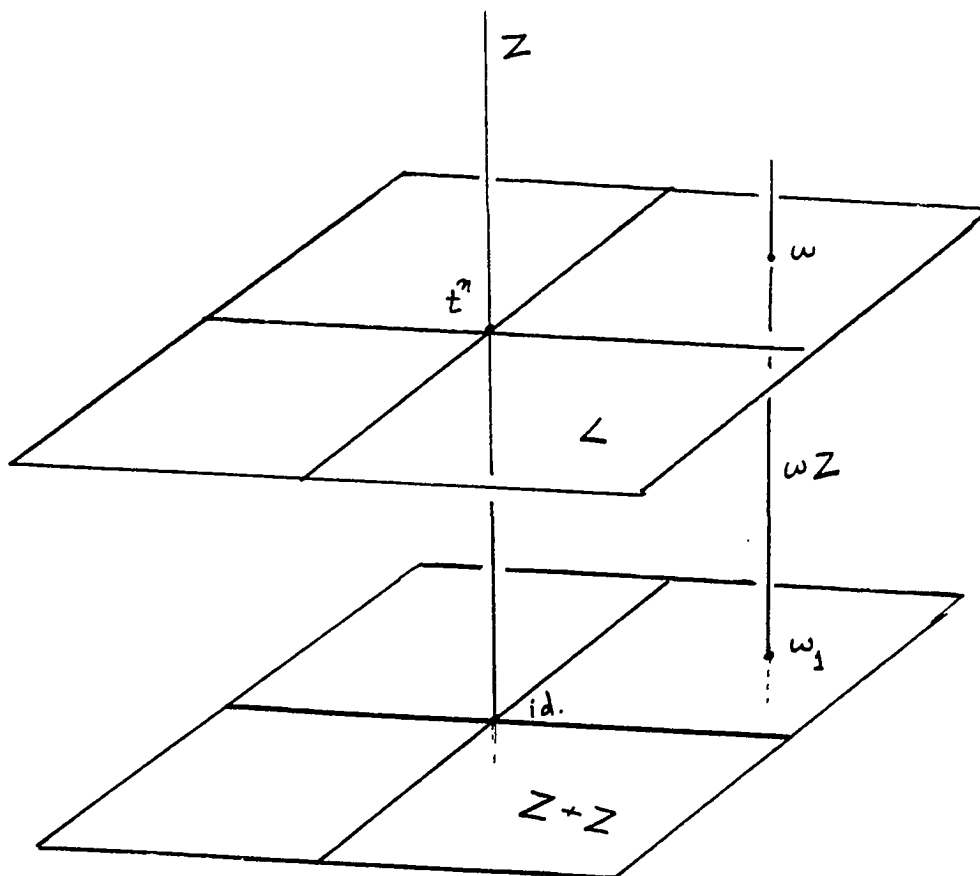
Thus the group generated by  $a$ ,  $b$  and  $tat^{-1}$  is free abelian of rank three.

Let us look at the words in  $G^\infty$  which, when abelianized, have no  $t$ 's in them. We study the group by studying the cosets of this subgroup.

## 4.2 TYPES IN A PLANE

We are looking at words in the group by looking first at words in cosets of the subgroup,  $H$ , of words whose abelianizations contain no  $t$ 's. For torus bundles, this subgroup is  $Z+Z$ . For the super group, it is  $Z^\infty$ . In either case, we can separate the words in a given coset of this subgroup into types which depend on how the word got there in the first place.

Let  $w$  be a word in a coset  $L$  of  $Z+Z$ . Consider the coset  $wZ$  of the subgroup generated by  $t$ . This coset intersects  $H$  at some element  $w_1$ . We call  $w_1$  the type of  $w$ .



It is much easier to talk about elements of a coset as if they were group elements. This naming allows us to do just that. Now for types, we can set

$$T(w_1) = tw_1t^{-1}.$$

In a torus bundle group,  $T(w_1)$  is still an element of  $Z+Z$ . In the super-group, it represents a new object in  $H$  which still commutes with  $a$  and  $b$ . We still call this a type, the type of  $T(w_1)$ . We can form higher order types by taking:

$$T^n(a) = t^n a t^{-n}.$$

Let us do layer  $h$ , that is, the coset of  $Z+Z$  which contains the word  $t^h$ . Note that words in layer  $h$  are in 1-1 correspondence with types. At time  $h$ , only the type of the identity shows up (the word  $t^h$ ). At time  $h+1$ , we get all the words  $at^h$ ,  $tat^{h-1}$ ,  $t^2at^{h-2}, \dots, t^h a$ , and the corresponding  $a^{-1}$ ,  $b$ , and  $b^{-1}$  versions. These are the types  $a$ ,  $T(a)$ ,  $T^2(a), \dots, T^h(a)$ , and similar names for the others, where

$$T^i(a^{-1}) = -T^i(a)$$

At time  $h+2$ , the types which appear are the sums of any two types of words which appeared at time  $h+1$ . That is,  $T(a) + T(b)$ ,  $T^2(a) - T^3(a)$ ,  $2T^5(a)$ , etc. Note that types commute. At time  $h+3$ , we get the expected sums of three types from time  $h+1$ , but we also get some new types. These correspond to words like  $t^{-1}at^{h+1}$  and  $t^{h+1}at^{-1}$ . These, and their  $a^{-1}$ ,  $b$  and  $b^{-1}$  counterparts, are the types  $T^{-1}(a)$ , and  $T^{h+1}(a)$  etc. Now while it is true that, at time  $h+4$ , we will get types like  $T(a) + T^{h+1}(a)$  and  $T^4(b) - T^{-1}(a)$ , we will not get types like  $T^{-1}(a) + T^{h+1}(b)$ .  $t^4bt^{h-4}ta^{-1}t^{-1}$  is length  $h+4$ , but  $t^{-1}bt^{h+2}bt^{-1}$  has length  $h+6$ . The moral is, types  $T^0$  through  $T^h$  will start generating sums like generators for an abelian group of rank  $h+1$  from the very start, even with the new types like  $T^{-1}$  and  $T^{h+1}$ , but not all new types will combine as readily. The rule is:

#### 4.2.1 Lemma

Let  $w = \sum_{j=-i}^{h+k} n_j T^j(\square)$ , where  $\square$  is a wild card, i.e.,  $a$  or  $b$ . Then  $w$  appears at time  $h$  plus

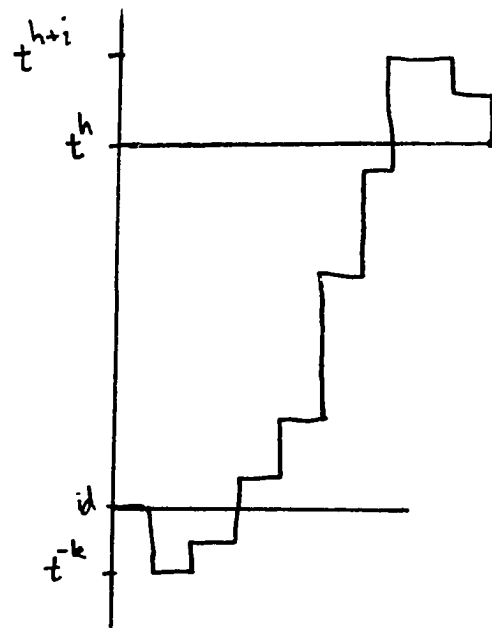
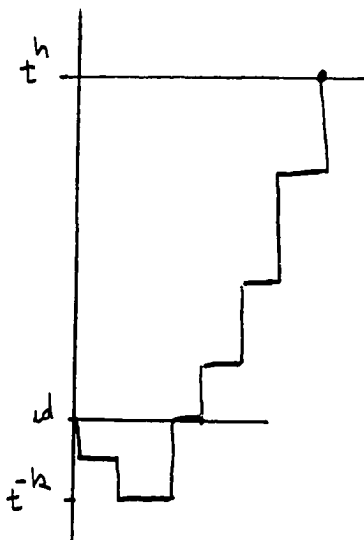
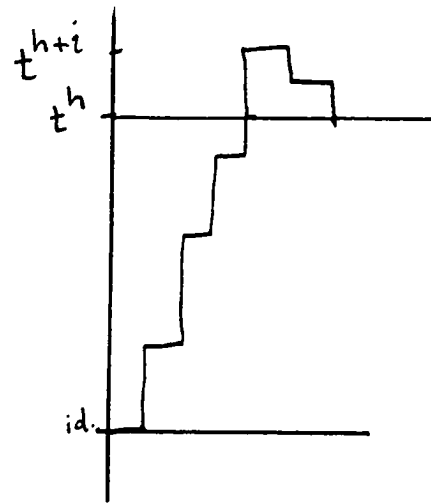
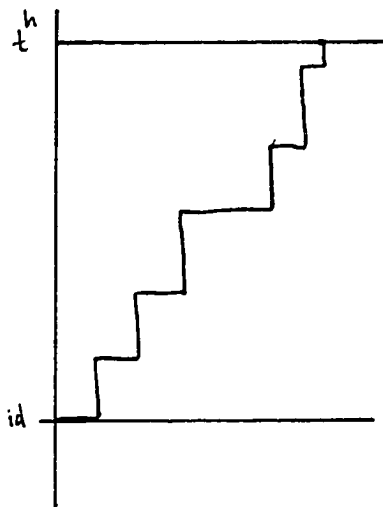
$$\sum_{l=0}^h n_l, \text{ if } k = i = 0,$$

$$\sum_{l=-i}^h n_l + 2i + 1, \text{ if } k = 0, i > 0,$$

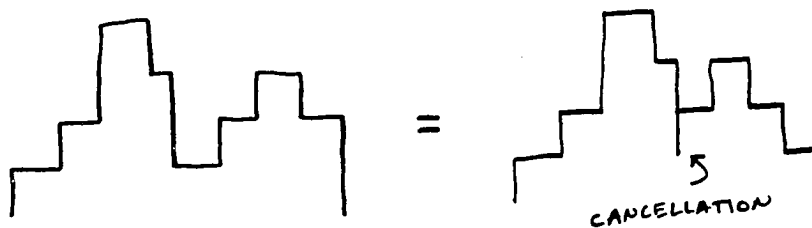
$$\sum_{l=0}^{h+k} n_l + 2k + 1, \text{ if } i = 0, k > 0,$$

$$\sum_{l=-i}^{h+k} n_l + 2k + 2i + 2, \text{ if } i > 0, k > 0.$$

The factors of 2 and the extra 1 or 2 come from overshooting the layer  $h$  and turning round.



Proof: Note that there are never more than two sign changes of the exponent of  $t$  in any word which has minimal length for the group element which it represents. That is, the word  $t^2 a t^{-5} b a^2 t^4 b^{-1} t^{-2}$  of length 18 is equal to the word  $t^2 a t^{-1} b^{-1} t^{-4} b a^2 t^2$  of length 14 because  $t^{-4} b a^2 t^4$  commutes with  $b^{-1}$ . In general, if there are more than two sign changes, the word can be shortened by commuting the bumps around.



The formulas then follow from inspection.

We are now in a position to calculate the growth function for the super group  $G^\infty$ . At layer  $h$  (the coset  $L_h = Ht^h$ ), first consider words whose types are of the form

$$\sum_{j=0}^k n_j T_j^j(\square), \quad n_k \neq 0.$$

for some fixed  $k$ . By the above formulas, we can see that the number of such types grows as those words in a free abelian group of rank  $2k+2$  which do not belong to the subgroup generated by the first  $2k$  generators. So if

$$\phi(s) = (1+s)/(1-s),$$

then the growth function for types of order k is:

$$\bar{\phi}_k(s) = (\phi^{2k+2}(s) - \phi^{2k}(s)) .$$

Now, at layer h, we have  $2h+2$  generators at time h. Then at time  $h+3$  we add 2 more (we are only counting types  $T^i$ ,  $i \geq 0$ ). At every other time unit, we add two generators, so we sum:

$$\begin{aligned} & s^h \phi^{2h+2}(s) + s^{h+2} \bar{\phi}_{h+1}(s) + s^{h+4} \bar{\phi}_{h+2}(s) + \dots \\ & + s^{h+2n} \phi_{h+n}(s) + \dots \end{aligned}$$

The exponents of s are due to the fact that when  $\bar{\phi}(s)$  was computed, the constant term was lost, so the extra power of s is absorbed in the coefficient.

This sum equals:

$$\frac{s^h (1-s)^3 (1+s)}{(1-2s-2s^3-s^4)}$$

Now we look at types  $T^j(a)$ ,  $T^j(b)$ ,  $j < 0$ . Any word in layer h has a non-negative part and a negative part. Let  $w$  = some word in layer

h. Then  $w$  is some sum of types. We can write  $w = w^+ + w^-$  where

$w^+$  = the sum of the types in  $w$  with  $T^j(\square)$ ,  $j \geq 0$

$w^-$  = the sum of types in  $w$  with  $T^j(\square)$ ,  $j < 0$ .

Now the time of occurrence of  $w$  is equal to the sum of the times of occurrence of  $w^+$  and  $w^-$ . Therefore, the delay between the occurrences of  $w^+$  and  $w$  depends only on  $w^-$ . Therefore, the generating function for the full group is the product of the generating function for the  $w^+$  with (1 + the generating function for the  $w^-$ .) At any positive layer, the  $w^-$ 's appear first at time  $h+3$ , with two generators, and then two more are added every other time. Thus the formula for the  $w^-$  at level  $h$  is

$$s^{h+2} \{ \bar{\phi}_0(s) + s^2 \bar{\phi}_1(s) + \dots + s^{2n} \bar{\phi}_n(s) + \dots \}$$

Which equals:

$$\frac{4s^{h+3}}{1-2s-2s^3-s^4}$$

So the full generating function for level  $h$  is

$$\left( \frac{(1-s)^3(1+s)}{(1-2s-2s^3-s^4)} \right)^2 \left( \frac{1+s}{1-s} \right)^{2h+2}$$

By symmetry, level  $h$  and level  $-h$  have the same generating function, so summing over layers yields:

$$\frac{(1+s)^4(1-s)^4(1-s+3s^2+s^3)}{(1-2s-2s^3-s^4)^2(1-3s-s^2-s^3)}$$

Note: The factor in the denominator with the smallest root is

$$1 - 3s - s^2 - s^3.$$

This comes from the last summing step. In each new layer, we get two new generators with each time unit, that is, at layer  $h$  we have  $2h+2$  generators to start, but at layer  $h+1$ , only one unit later, we have  $2h+4$ . Within each layer, we get new generators every two time units, and that accounts for the larger roots of the other denominator factor.

### 4.3

#### THE SIMPLIFICATION

Every torus bundle group has a subgroup of finite index which is much simpler for our purposes. Let  $G$  be the fundamental group of a torus bundle over a circle with generators  $a$ ,  $b$ , and  $t$  as above. For every non-trivial element  $x$  in  $Z+Z$ , there is a sublattice of finite index generated by  $x$  and  $T(x)$ . The matrix  $\Psi$  acts on this sublattice by

$$\begin{array}{cc} 0 & -1 \\ \vdots & \vdots \\ 1 & \text{Trace}(\Psi) \end{array}$$

Now our calculations are much simpler. This corresponds to looking at the growth function of the fundamental group of a finite cover of our original torus bundle. The advantage of this simplification is that only one half as many new types appear at any one time. In fact, as  $T(a) = b$ , and  $T(b) = T^2(a)$ , we need never talk about  $b$ 's at all. There is a super group for torus bundles of this type which has a smaller growth rate than the super group  $G^\infty$ . It is generated by  $a$ ,  $b$ , and  $t$ , with relations

$$\{a, b, t \mid [a, b] = \text{id}, tat^{-1} = b, [a, tbt^{-1}] = \text{id}, [b, tbt^{-1}] = \text{id}.\}$$

Its growth function is calculated in a similar manner to  $G^\infty$ . The answer is

$$\frac{(1+s)^4(1-s)^2(1+s^2)}{(1-s-s^2-s^3)^2(1-2s-s^2)}$$

Now we do an actual torus bundle. Let us do the case  $\text{Trace}(\Psi) = 4$ , as this will generalize to all even traces. As before, we will look first at words in a given layer with only positive types.

Definition: The age of a word at time  $s$  is the difference ( $s$  - the time at which that element first appeared.) The objects of study will be the appearance of new words between two older words, both of which are of comparable age and type, for instance,  $3T^4(a)$  and  $T^5(a)$  are always of the same age, and are nearly of the same type. As time passes, the space between these two words fills with their progeny.

EXTREMELY IMPORTANT POINT : The offspring of two parent words always stay between them.

For instance, The offspring of  $T^4(a)$  which threaten most to get away are  $2T^4(a)$ ,  $3T^4(a)$ , etc.  $T^4(a)$  is so much bigger than  $T^3(a)$ , that the  $T^3(a)$ 's do not threaten to invalidate the extremely important point. But look, the first one to get beyond  $T^5(a)$  is  $4T^4(a)$ . This, however, is equal to  $T^5(a) + T^3(a)$ , since

$$T^n(a) - \text{Trace}(\Psi)T^{n-1}(a) + T^{n-2}(a) = 0$$

So the space between them is the whole battlefield.

Fix a layer  $h$  in which we will work. We will have to understand the development of words in three different situations. The cases are when the parent points are:

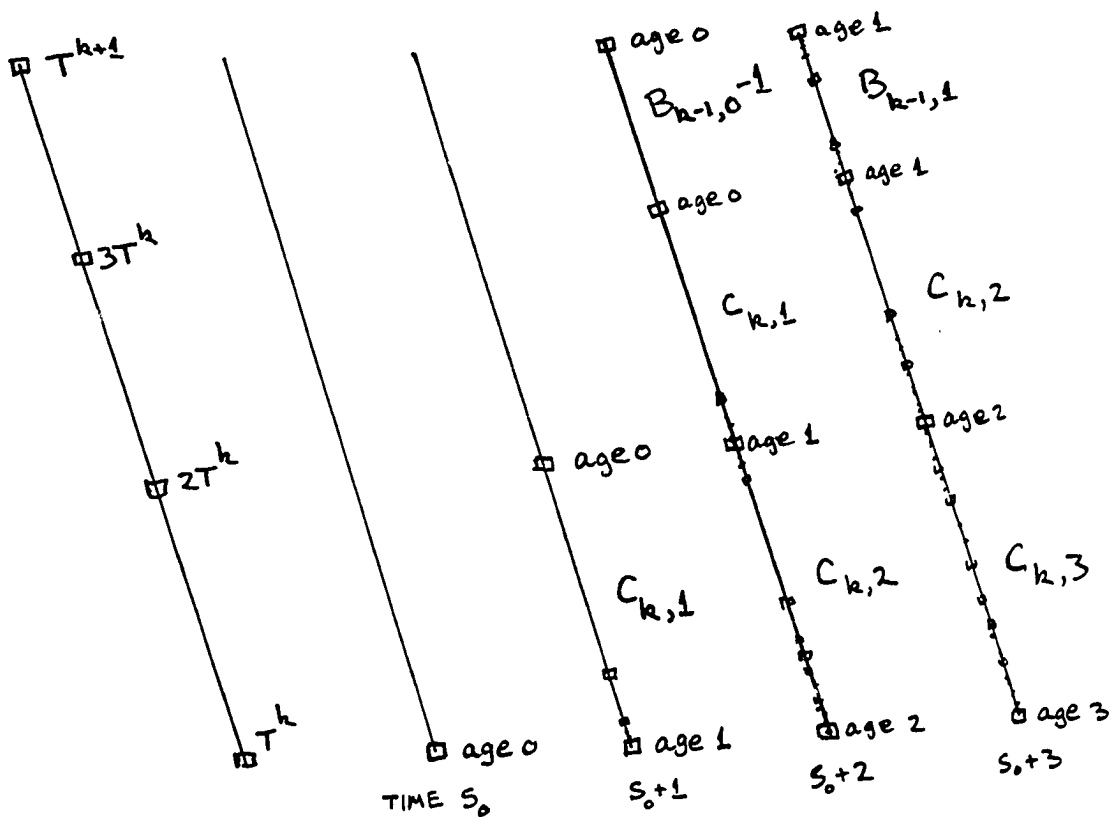
1.  $T^k(a)$  at age 2 and  $T^{k+1}(a)$  at age 0
2.  $T^k(a)$  at age 0 and  $T^{k+1}(a)$  at age 0
3.  $T^k(a)$  at age 1 and  $2T^k(a)$  at age 0.

Let  $A_k(s)$ ,  $B_k(s)$ , and  $C_k(s)$  be the generating functions for the number of words formed between the parent points in each of the above situations, that is,

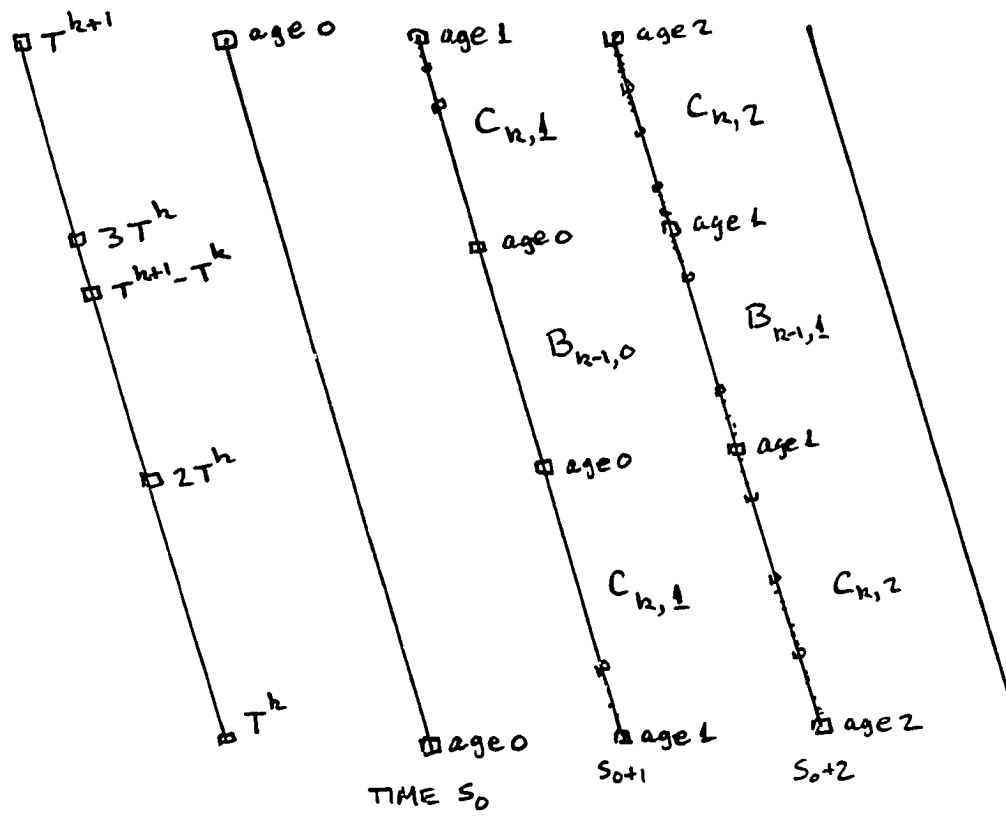
$$A_k(s) = A_{k,0} + A_{k,1}s + A_{k,2}s^2 + \dots$$

and  $A_{k,0} = 1$ ,  $B_{k,0} = 2$ , and  $C_{k,0} = 1$ .

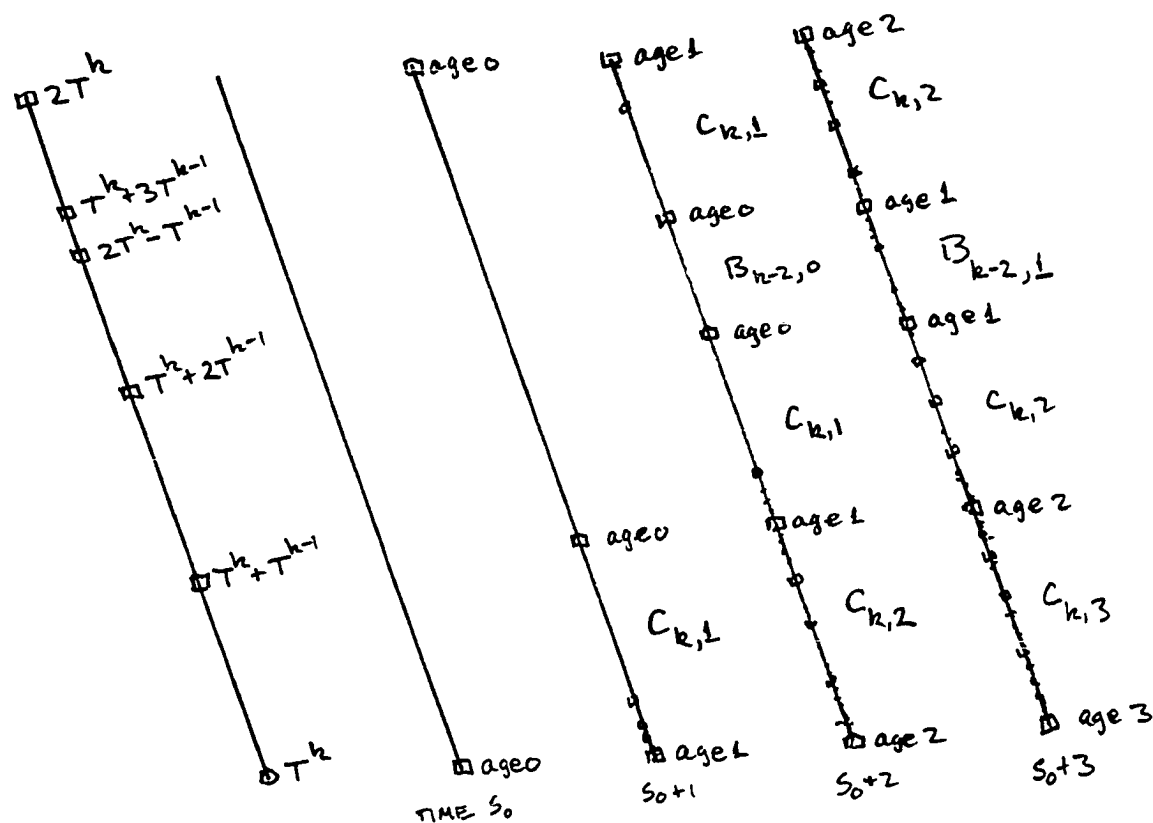
We get a lot of recursion,



$$A_k(s) = C_k(s) + sC_k(s) + t^2(B_{k-1}(s) - 1)$$



$$B_k(s) = 2C_k(s) + sB_{k-1}(s)$$



$$C_k(s) = C_{k-1}(s) + 2sC_{k-1}(s) + s^2B_{k-2}(s)$$

From this, we conclude that

$$C_k(s) = C_{k-1}(s) + 3sC_{k-1}(s) - sC_{k-2}(s)$$

To sum up layer  $h$ , we start at time  $h$  with the identity. At time  $h+1$ , we get the  $h$  types  $a, T(a), T^2(a), \dots, T^h(a)$ . The words between each of these are given by the functions  $B_k(s)$ . In particular,

$$\sum_{i=1}^{h-1} (B_i(s)-1)$$

After that, at time  $h+3$ , we get  $T^{h+1}(a)$ .  $T^h(a)$  is age 2, so the points in between them were growing as  $A_h(s)$  since time  $h+1$ . At time  $h+5$ , the type  $T^{h+2}(a)$  appears, and so we have the words between  $T^{h+1}(a)$ , age 2, and  $T^{h+2}(a)$ , age 0, which means we had an  $A_{h+1}(s)$  starting at time  $h+3$ . At times  $h+2n+1$ , we will get a new  $A_{h+n}(s)$ . Therefore, the growth of positive types in layer  $h$  is given by

$$s^h \left( 1 + s \sum_{i=1}^{h-1} (B_i(s)-1) + \sum_{n=1}^{\infty} s^{2n+1} A_{n+h}(s) \right)$$

The words of negative type are computed in a similar manner, following the same reasoning as for the super-group  $G^\infty$ . The growth of a layer really is the product of the growths of the types  $T^i(a)$ ,  $i > 0$ , and the types  $T^j(a)$ ,  $j \leq 0$ .

The growth for layer  $h$  is then given by:

$$s^h \left( 1 + \sum_{i=1}^{h-1} (B_i(s)-1) + \sum_{n=1}^{\infty} s^{2n+1} A_{n+h}(s) \right) \left( 1 + \sum_{m=1}^{\infty} s^{2m+1} A_m(s) \right)$$

By tedious manipulations of the recursions among A, B, and C, we can show that the growth function in question is rational with denominator:

$$(1 - s - 3s^2 + s^3)(1 - s^2 - 3s^3 - s^5)^2(1 - s)^4$$

The reason for this is that upon multiplying by  $(1-s)^4$ , the expression for the growth function involves only terms of the form

$$\sum_{i=1}^{\infty} s^i C_i(s), \text{ and } \sum_{i=1}^{\infty} s^{2i} C_i(s).$$

The recursion among the C's gives the above denominators as the denominators of rational functions for these two sums.

For other even traces, the recursions among the A's, B's, and C's are similar. We have:

$$C_n(s) = (1+2s+2s^2+\dots+2s^{k-2}+3s^{k-1})C_{n-1}(s) - s^{k-1}C_{n-2}(s)$$

Where  $k = (1/2)\text{Trace}(\Psi)$ .

The denominator of the growth function will be:

$$(1-s-2s^2-2s^3-\dots-2s^{k-1}-3s^k+s^{k+1})(1-s^2-2s^3-\dots-2s^k-3s^{k+1}-s^{k+3})^2(1-s)^4$$

For odd trace, the recursion among the A's, B's, and C's is different, but it can be done. It will have to wait until next time.

It is interesting at this point to take the limits as the traces get large. We see that the denominators of the growth functions converge to the denominator of the growth function for the simplified supergroup.

## Chapter V

### SL(2,R) AND SEIFERT FIBRE SPACES

Another of the 3-manifold geometries is called  $SL_2$ . It is modelled on the universal cover of the group  $SL_2\mathbb{R}$ . This can also be thought of as the universal cover of the unit tangent bundle of the hyperbolic plane. It is by the projection  $p:T_1H^2 \rightarrow H^2$  that the isometries of  $SL_2$  are understood. The isometries of  $H^2$  lift to a normal codimension 1 subgroup of  $\text{Isom}(SL_2)$ . Every non-trivial Seifert fibred space whose base orbifold has negative Euler characteristic can be modeled on this geometry.  $SL_2$  has the following properties: The subgroup of isometries which fix a given point also fixes a line through that point. The resulting foliation of  $SL_2$  by lines has a transverse hyperbolic metric. The 2-plane distribution orthogonal to this foliation is not integrable. For more information on  $SL_2$ , refer to Scott[10].

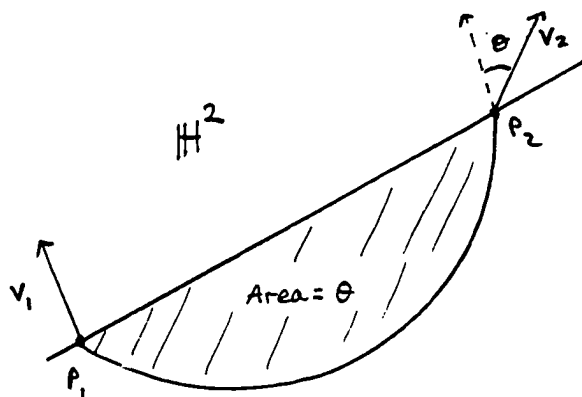
#### 5.1 ISOMETRIES OF $SL_2$

The group  $SL_2\mathbb{R}$  acts on  $SL_2$  without fixed points by a lifting of its action on the hyperbolic plane. The full group  $\text{Isom}(SL_2)$  is a normal extension of  $SL_2\mathbb{R}$  by  $\mathbb{R}$ . The  $\mathbb{R}$  corresponds to a 1-parameter subgroup of isometries of  $SL_2$  which do not arise as lifts of motions of the hyperbolic plane. Think of the unit tangent bundle to the hyperbolic

plane. There are two kinds of isometries which are easy to see. There are isometries of the hyperbolic plane, which lift to isometries of the unit tangent bundle, and there are isometries which leave fixed the plane but which rotate each tangent vector through a constant angle. Neither of these two types of isometries have fixed points, but there is a combination which does. Consider an elliptic hyperbolic isometry which rotates about a point  $p$  by an angle  $\theta$ . Now, fix the plane and rotate each tangent vector through the angle  $-\theta$ . The composition isometry fixes the set of tangent vectors at  $p$ , but has no other fixed points.

Note: What is really happening is that we are choosing a 2-plane distribution of the frame bundle of the plane so that the plane may have constant negative curvature.

We can now define a metric which is preserved by the above group of isometries. It is made possible by the local non-integrability of the distribution orthogonal to the fixed lines of isometries. To find the distance between two points in  $SL_2$ , look at their representations as unit tangent vectors to the hyperbolic plane. Their distance is the length of the shortest path in  $H^2$  between their base points with the property that parallel translation along that path will take one vector to the next. It is easy to see that such a path is always a circular arc whose area is the difference in the angles of the two vectors.



This metric is equivalent to the degenerate Riemannian metric obtained by preserving the hyperbolic metric on the horizontal directions while letting the vertical distances increase to infinity. That is, the only paths which have a hope of being finite in length must stay tangent to the horizontal distribution. In general, given a path in  $SL_2$  orthogonal to the foliation of fixed lines, its length is exactly the length of its projection to the hyperbolic plane. Conversely, given a path in  $H^2$ , it has a unique horizontal lift to  $SL_2$ . If the path is a  $C^1$  closed loop in  $H^2$ , then the endpoints of the lifted path will lie on the same vertical line. Since the curvature of  $H^2$  is  $-1$ , the two endpoints will differ by a rotation of  $-(\text{Area enclosed by the loop downstairs})$ . If the loop is piecewise  $C^1$ , then it lifts to a union of paths with vertical breaks corresponding to the exterior angles at the corners.

## 5.2 AN IRRATIONAL SUBGROUP

We will look at the fundamental group of a 3-manifold modelled on  $SL_2$ . A good candidate is the Euler class 1 circle bundle over the surface of genus 2. (This is the double cover of the unit tangent bundle to the surface.) The fibration

$$S^1 \rightarrow M \rightarrow S_2$$

induces

$$0 \rightarrow \pi_1(S^1) \rightarrow \pi_1(M) \rightarrow \pi_1(S_2) \rightarrow 0.$$

The last projection we call  $p$ . The fundamental group of  $M$  is generated by five elements and their inverses. Four elements project down to the generators for the fundamental group of the surface, and the remaining one generates the kernel of the projection. The group is

$$\{a, b, c, d, t \mid [a, b][c, d] = t, [a, t] = \text{id}, [b, t] = \text{id}, \text{etc.}\}$$

There is an obvious representation of this group on the isometries of  $SL_2$ .  $a$ ,  $b$ ,  $c$  and  $d$  lift as do all hyperbolic isometries. The element  $t$  corresponds to a vertical translation by the area of a surface of genus 2, that is,  $4\pi$ .

Now, note that we do not need to include  $t$  in our list of generators for the group  $G$ . We can instead define the fundamental group as

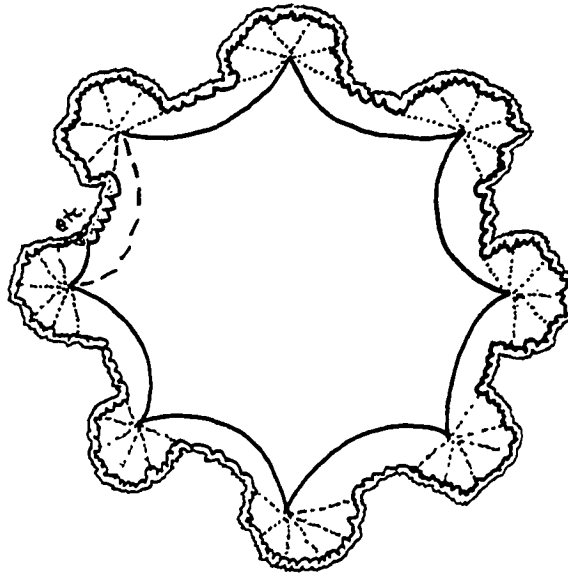
$\{a,b,c,d \mid [[a,b],[c,d]]=id., \text{ and other appropriate permutations}\}$

Now we ask the question: what is the generating function for the growth of elements in  $Z$  which is the kernel of the projection  $p$ , given that we take only  $a, b, c$  and  $d$  as generators? The answer is an irrational function.

To determine the occurrences of group elements in  $\ker(p)$  it suffices to look at the graph  $\Gamma$  of the fundamental group for the surface of genus 2. Every path in the graph starting at the identity corresponds to an element of  $G$ . Two paths correspond to the same element of  $G$  iff they enclose zero signed area. An element of  $\ker(p)$  corresponds to a closed path through the identity. The length of time that it takes an element  $k$  of  $Z$  to be counted by the growth function is equal to the minimum perimeter of a collection of  $k$  octagons in the graph  $\Gamma$ . To answer the question of the relation of perimeter to area for a collection of octagons, we introduce the Fundamental Spiral of the graph  $\Gamma$ .

### 5.2.1 The Fundamental Spiral

Definition: The fundamental spiral  $\Sigma$  is defined inductively. Start at any point in  $\Gamma$  and connect it to one of its neighbors. Now the rule is: always add the right most edge. The only condition is that you never complete a loop.



### 5.2.2 Theorem

The fundamental spiral is a maximal tree for the graph  $I$  with the property that any closed path obtained by adding a complementary branch has the minimum perimeter for its area. Furthermore, every area appears in this way.

Proof by induction: Consider  $k$  octagons in the plane. Assuming the obvious choice of a simply connected arrangement for minimum perimeter, we have by the Gauss-Bonnet theorem,

$$\text{Area} = \text{Sum of the Exterior Angles} - 2\pi.$$

We can count the vertices on the perimeter two different ways: one with multiplicity, the other without. Let  $V_m^P$  be the number of vertic-

es on the perimeter counted with multiplicity. Let  $V^P$  be the number of vertices on the perimeter counted without multiplicity. Notice that  $V^P$  is equal to the number of edges on the perimeter. Let  $V^i$  be the number of vertices in the interior, and let  $V_m^i$  be the number of vertices in the interior counted with multiplicity. We now have the following formulas:

$$\text{Area} = 4\pi k = \pi V^P - (\pi/4)V_m^P - 2\pi$$

$$V_m^P = 8k - V_m^i$$

or, since

$$V_m^i = 8V^i,$$

$$V_m^P = 8k - 8V^i$$

therefore, we have:

$$\text{Area} = \pi V^P + 2\pi V^i - 2\pi(k+2)$$

Therefore, to minimize the perimeter, or maximize the area, we must maximize the number of interior vertices,  $V^i$ . Geometrically, this is completely reasonable.

In order to study the vertices in the interior of the graph, we introduce the dual reduction.

### 5.2.3 The Dual Reduction of an Octagon Packing

Suppose that we have  $k$  octagons arranged so that their union is a disk. The  $k$  octagons form a planar graph  $\gamma$  in  $\Gamma$ . The dual reduction  $\gamma^*$  is a subgraph of the dual graph  $\Gamma^*$  of  $\Gamma$ .  $\gamma^*$  has one point for each octagon of  $\gamma$ . Two points in  $\gamma^*$  are connected by an edge iff their preimages in  $\gamma$  have an edge in common. Inside  $\gamma^*$  is a subgraph  $\gamma_0^*$  consisting of those vertices and edges which are parts of complete octagons in  $\gamma^*$ .

### 5.2.4 Lemma

Let  $\gamma$  be an optimal arrangement of  $k$  octagons. Then  $k > 7$  implies  $\gamma^* - \gamma_0^*$  consists of six or less vertices.

Proof: Eight octagons must be arranged with a common vertex to be optimal. (Obvious, or Exercise) Thus if  $\gamma^*$  has eight vertices, then  $\gamma^* = \gamma_0^*$ . Now suppose that  $\gamma^* - \gamma_0^*$  contains seven or more vertices. Each vertex corresponds to an octagon in  $\gamma$  which has no vertex in the interior. Thus, if these octagons are removed and rearranged, another interior vertex can be added to  $\gamma$ , contradicting the optimality of  $\gamma$ .

Notice that we have no control over  $\gamma^* - \gamma_0^*$ . Any rearrangement of the octagons in  $\gamma$  corresponding to  $\gamma^* - \gamma_0^*$  will also be optimal. This is because none of the octagons in  $\Gamma$  have any interior vertices, and there are not enough of them to create any new interior vertices. Let  $\gamma_0$  be the set of octagons corresponding to  $\gamma_0^*$ . Then  $\text{per}(\gamma) = \text{per}(\gamma_0) + 6\#(\gamma^* - \gamma_0^*)$ . We thus conclude:

$$\gamma \text{ optimal} \Leftrightarrow \gamma_0 \text{ optimal.}$$

We need just two more steps. First, we wish to show that  $\gamma_0^*$  optimal implies  $\gamma_0$  optimal. Second, we need that if  $\gamma$  represents a cycle from the Fundamental Spiral, then  $\gamma_0^*$  does as well. This, together with the fact that for all  $k$ , there exists an edge in the complement of the Fundamental Spiral such that the cycle it defines has area  $k$ , will prove the main assertion.

Step 1:  $\gamma_0^*$  optimal  $\Rightarrow$   $\gamma_0$  optimal.

If  $\gamma_0^*$  is optimal, then it has the greatest number of interior vertices for its area and the greatest area for its number of vertices. This follows from the formula above. But the number of octagons in  $\gamma_0^*$  is equal to the number of interior vertices in  $\gamma_0$ . And the number of vertices of  $\gamma_0^*$  is equal to the number of octagons of  $\gamma_0$ . Therefore,  $\gamma_0$  has the greatest number of interior vertices for a fixed number of octagons, hence it is optimal.

Step 2:  $\gamma$  from the Fundamental Spiral      $\gamma_0^*$  from the Fundamental  
Spiral.

I leave this as an exercise. Look carefully at the graph of the  
Fundamental Spiral.

To complete the proof of irrationality, we need

### 5.2.5 Lemma

Let  $\{a_i\}$  be a sequence of integers with rational generating function with the property that  $a_i < ci$  for some constant  $c$ . Then there exists integers  $M$  and  $k$ , and rational numbers  $r_1, \dots, r_M$ , such that

$$a_{i+kM} = a_i + kr_i, \quad 0 < i < M+1.$$

In particular, if the  $a_i$  are an increasing sequence, then the  $r_j$  are all equal, and the limiting slope  $a_i/i$  is rational.

Proof: Consider the denominator,  $q(s)$ , for the generating function for the  $a_i$ . Since the  $a_i$  are integers, the roots of  $q(s)$  must be the inverses of algebraic integers. The linear growth condition on the  $a_i$  imply that  $q(s)$  has no roots inside the unit circle. Therefore, all of the roots of  $q(s)$  lie on the unit circle. But an algebraic integer all of whose conjugates lie on the unit circle must be a root of unity. See Borevich and Shafarevich[2], pg. 89. Let  $M$  be the least common multiple of the orders of the roots of  $q(s)$ . Then the lemma follows by induction on the number of roots of  $q(s)$ . Let  $\zeta$  satisfy  $\zeta^M = 1$ . Then let

$$q'(s) = (s-\zeta)q(s).$$

Let  $\{b_i\}$  be the coefficients of  $p(s)/q'(s)$ . Then

$$b_i = a_i + a_{i-1}\zeta + a_{i-2}\zeta^2 + \dots + a_0\zeta^i$$

So we have

$$b_{i+kM} = b_{i+(k-1)M} + \text{a term which depends only on } i \\ + \text{a constant times } k.$$

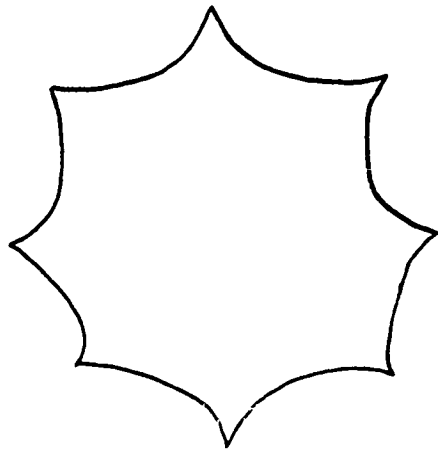
The last term must be zero if we are to have linear growth. The lemma follows.

Now, if we set

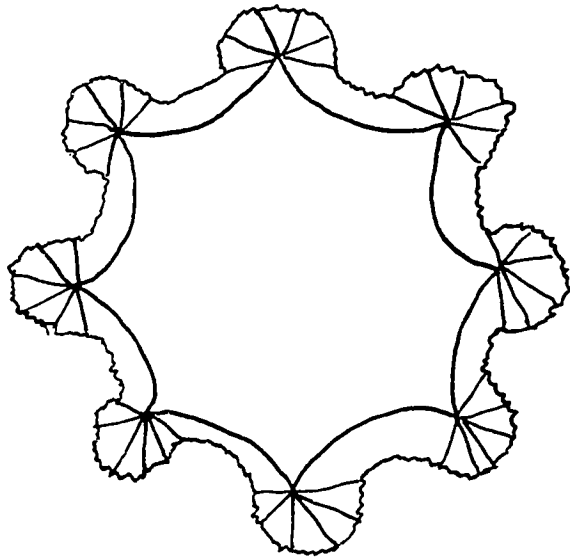
$a_i$  = the number of octagons which can be arranged to have perimeter less than or equal to  $i$ ,

then, for the  $a_i$  to be given by a rational generating function, the limit of  $a_i/i$  would have to be a rational number. This is the limit of the ratio of area to perimeter for optimal octagon packings. But we can calculate the area and perimeter of large loops in the Fundamental Spiral, and we will see that the ratio of area to perimeter is not rational in the limit.

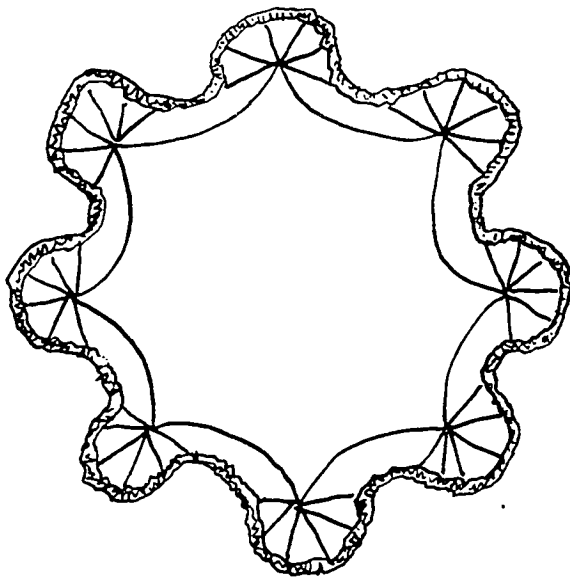
Look at the following layers in the fundamental spiral.



Layer 1



Layer 2



Layer 3

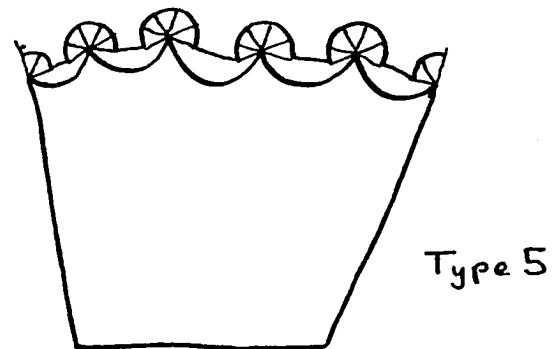
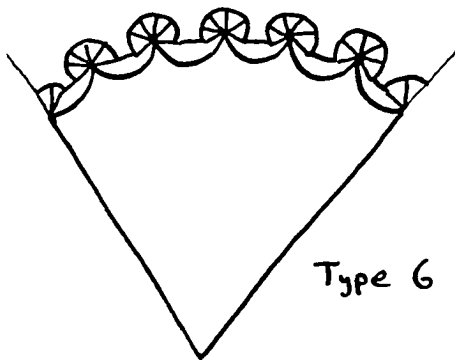
etc.

The two kinds of behaviour on the boundary of each layer are an octagon with six edges on the boundary, and an octagon with five edges on the boundary. Call these type 6 and type 5 octagons respectively.

The recursion between layers gives a matrix

$$\begin{matrix} 29 & 24 \\ 6 & 5 \end{matrix}$$

$$\begin{matrix} 6 & 5 \end{matrix}$$



The initial condition vector is 40 of type 6 and 8 of type 5. In the limit, this converges projectively to the eigenvector

$$\lambda-5$$

$$6$$

Where  $\lambda$  is a root of

$$\lambda^2 - 34\lambda + 1 = 0.$$

Now the perimeter at a given layer is 6 times the number of type 6 octagons plus 5 times the number of type five octagons in that layer. The area enclosed by a layer approximates  $\lambda$  times the number of octagons in that layer.

$$\text{Perimeter approaches } 6\lambda^n(\lambda-5) + 5\lambda^n(6)$$

$$\text{Area approaches } \lambda^n(\lambda-5) + \lambda^n(6)$$

So we see that the ratio of area to perimeter is

$$(\lambda+1)/6\lambda$$

which is not rational.

## BIBLIOGRAPHY

- [1] Benson, Max. Growth Series of Finite Normal Extensions of  $Z$  Are Rational. Preprint, (1982).
- [2] Borevich, Z.I. ad Shafarevich, I.R. Number Theory Academic Press, (1966).
- [3] Bourbaki, N. Groupes et Algebres de Lie. Chapitres 4,5, et 6, Paris, Hermann, (1968).
- [4] Cannon, James W. The Growth of the Closed Surface Groups and the Compact Hyperbolic Coxeter Groups. Preprint.
- [5] Cannon, James W. The Combinatorial Structure of Cocompact Discrete Hyperbolic Groups. Geometriae Dedicata, to appear.
- [6] Gromov, M. Groups of Polynomial Growth and Expanding Maps. Publ. Math. I.H.E.S. 53, (1981).
- [7] Menasco, W. Incompressible Surfaces in the Complement of Knots and Links. Preprint.
- [8] Milnor, J. A Note on Curvature and Fundamental Group. J. Differential Geometry, 1 (1968), 1-7.
- [9] Milnor, J. Growth of Finitely Generated Solvable Groups. J. Differential Geometry, 2 (1968), 447-448.
- [10] Scott, P. The Geometries of 3-Manifolds. Preprint.
- [11] Spivak, M. A Comprehensive Introduction to Differential Geometry. Second edition, Publish or Perish Press (1979).
- [12] Thurston, W.P. Three Dimensional Geometry and Topology. Princeton University Press, to appear.
- [13] Wolf, J.A. Growth of Finitely Generated Solvable Groups and Curvatures of Riemannian Manifolds. J. Differential Geometry 2 (1968), 421-446.